Design and Performance Studies on Single-Mode Optical Fiber Cable(Dissertation_全文)

AUTHOR(S):

Katsuyama, Yutaka

DESIGN AND PERFORMANCE STUDIES ON SINGLE-MODE OPTICAL FIBER CABLE

by
YUTAKA KATSUYAMA

Ibaraki Electrical Communication Laboratory,
Nippon Telegraph and Telephone Public Corporation.
(November 1980)

CONTENTS

CHAPTER I INTRODUCTION

Optical communication has attracted special interest since laser oscillation was succeeded in 1960 and low-loss (20 dB/km) optical fiber was fabricated [1] in 1970. A large number of studies on fiber fabrication technique resulted in lowering the transmission loss, and ultra low-loss characteristics smaller than 1 dB/km were attained for multi-mode fiber [2] and for single-mode fiber [3]. As a result, it was found that optical fiber made of fused silica was extremely attractive transmission medium.

Optical fibers are classified into two types; multi-mode fiber and single-mode fiber. Only the lowest mode, HE_{11} mode, can propagate in the single-mode fiber. Therefore, transmission capacity is large. However, it is rather difficult to splice single-mode fibers, because of the small core diameter (5 - 15 μm). On the other hand, multi-mode fibers have smaller transmission capacity, and it is relatively easy to splice them. It is expected that single-mode fibers are fully utilized as future transmission medium, by making the most use of the excellent transmission characteristics.

Suitable cable structure and manufacturing technique are required to prevent the mechanical failure of the glass fibers, because they are made of brittle material.

Furthermore, random stresses cause fiber bends and consequently loss increases. It is necessary to preserve the low-loss characteristics of optical fiber during cable manufacturing process and long term use. The main points for cable design are (1) enough mechanical strength and (2) stable transmission characteristics without loss increase.

At an early stage of cable investigations, multi-mode fibers were mainly treated. It was shown [4] experimentally that large loss increase occurred when an optical fiber was pressed on a rough surface. This is because the fiber bend occurs under pressure and gives rise to radiation loss due to random deflection of fiber axis from the original straightness. The loss increase which is called microbending loss is found to occur even due to small deflection of fiber axis. It is important to reduce the microbending loss for low-loss cable fabrication. Therefore, many studies were made for the microbending mechanism. The loss increses were measured for a fiber under lateral force [5], hydraulic pressure [6] and temperature change [5]. The results showed that cushion material was effective to reduce microbending loss. Therefore, many kinds of cables with appropriate arrangement of cushion layers were proposed and the fundamental characteristics were investigated [7].

Reports about single-mode fiber cables were very few, compared with those about multi-mode fiber cables. In this thesis, design and performance studies on a single-mode fiber cable are described.

Chapter II [8] describes cable design on the basis of optical loss characteristics evaluated experimentally. A cable containing eight single-mode fibers was manufactured and loss increase characteristics were examined. The existence of a wide V-value region without cabling loss increase has been shown clearly. The cabling loss increase depends on the relative index difference Δ. Therefore, suitable value of Δ has been determined so as to minimize cabling and splicing losses. As a result, it is fully possible to develop a single-mode fiber cable without loss increase.

Chapter III [9] describes strain characteristics of the optical cable under several external forces. Fiber strain inside the cable has been evaluated by a novel method (resistance wire method). In this method, strain is evaluated by measuring the resistance change of a metal wire coated with the same coating material for a glass fiber. It has been found that the method is simple and accurate. The measured results have verified that the cable has enough mechanical strength to install in the natural environment. The fiber strain in the cable is

much smaller than the failure strain of the silica fiber.

Chapter IV [10] describes transmission loss of a coated single-mode fiber at low temperature. The relation between loss increase and cooling strain due to coating contraction has been clarified. The cooling strain was measured by the resistance wire method described in Chap. III. Suitable diameter of the buffer layer has been determined for realizing negligibly small loss increases. As a result, buffer layer in a coated fiber is effective to prevent loss increase due to cooling. Therefore, it is expected that the cable containing the fibers coated with suitable buffer layer has the stable transmission characteristics at low temperature.

Appendices A [11], B [6], and C [12] are given to supplement the design of single-mode optical fiber cable, which is shown through Chap. II - IV.

References

1. F. P. Kapron, D. B. Keck, and R. D. Maurer: 'Radiation losses in glass optical waveguides', Appl. Phys. Lett., 17, 7, p.423 (1970)
2. M. Horiguchi, and H. Osanai: 'Spectral losses of low-OH content optical fibres', Electron. Lett., 12, 12, p.310 (1976)
3. A. Kawana, T. Miyashita, M. Nakahara, M. Kawachi, and T. Hosaka: 'Fabrication of low-loss single-mode fibres', Electron. Lett., 13, 7, p.188 (1977)
4. W. B. Gardner: 'Microbending loss in optical fibers', Bell Syst. Tech. J., 54, 2, p.457 (1975)
5. T. Naruse, Y. Sugawara, and K. Masuno: 'Nylon-jacketed optical fibre with silicone buffer layer', Electron. Lett., 13, 6, p.153 (1977)
6. Y. Katsuyama, S. Mochizuki, T. Yashiro, and Y. Ishida: 'Hydraulic pressure dependence of optical loss in jacketed optical fibre', Electron. Lett., 14, 12, p.372 (1978), See Appendix B.
7. K. Ishihara, M. Tokuda, and S. Seikai: '48 core optical fiber cable design and characteristics', Rev. Electr. Commun. Lab. NTT Jpn., 27, 11-12, p.949 (1979)
8. Y. Katsuyama, S. Mochizuki, K. Ishihara, and T. Miyashita: 'Single-mode optical fiber cable', Appl. Opt., 18, 13

p.2232 (1979)

9. Y. Katsuyama, Y. Mitsunaga, Y. Ishida, and K. Ishihara: 'Strain measurement in optical fiber cable using resistance wire', accepted in Japan. J. Appl. Phys.

10. Y. Katsuyama, Y. Mitsunaga, Y. Ishida, and K. Ishihara: 'Transmission loss of coated single-mode fiber at low temperatures', Appl. Opt., 19, 21, p. (1980)

11. Y. Katsuyama, M. Tokuda, N. Uchida, and M. Nakahara: 'New method for measuring V-value of a single-mode optical fibre', Electron. Lett., 12, 25, p.669 (1976)

12. Y. Katsuyama: 'Single-mode propagation in 2-mode region of optical fibre by using mode filter', Electron. Lett., 15, 14, p.442 (1979)

CHAPTER II SINGLE-MODE OPTICAL FIBER CABLE

Synopsis

A single-mode optical fiber cable was manufactured; loss increase characteristics due to cabling were evaluated. The existence of wide V-value regions without cabling loss increases is shown by a suitable selection of fiber parameters and optical wavelengths. A selection method for fiber parameters, which minimizes cabling and splicing loss increases, is discussed. Selected values are Δ=0.2 % and V=2.2, based on experimental results.

§1. Introduction

A single-mode optical fiber is an attractive transmission medium since it has broadband and low-loss [1] transmission characteristics. However, the optical loss of the fibers increases [2] due to various types of bends caused during cabling processes. In order to realize transmission systems using single-mode fibers, a low-loss cabling technique must be developed. Low-loss cable structures have been reported [3] for graded-index fibers. The main purpose of the structure is to prevent fiber bendings, causing loss increase. It is believed that the structures are also applicable to a single-mode fiber cable. It has been reported [4], for single-mode fibers, that the higher modes in an optical fiber show large attenuation near the cutoff wavelength. However, the loss increase characteristics are unclear during the processes of manufacturing a low-loss cable.

A cable containing eight single-mode fibers was manufactured, and loss increase characteristics were examined. In this chapter, some experimental results about cabling are reported. We shall show that it is possible to develop single-mode fiber cables without loss increase by the selection of the appropriate optical wavelength and fiber parameters.

§2. Cable Design on the Basis of Optical Loss

In the cabling process, optical fibers are usually coated with plastics, stranded, and sheathed. Optical loss increases occur during these processes; they depend on many parameters such as fiber parameters and cable structure. A cable structure was designed to obviate loss characteristics caused by cabling.

2.1 Optical fiber

The fiber parameters for the eight-fiber cable were chosen as follows. The relative refractive index difference Δ and core radius a must satisfy the single mode condition, which is represented by

$$V \simeq \frac{2\pi a}{\lambda} n_2 \sqrt{2\Delta} < 2.405, \qquad (1)$$

where V is the normalized frequency (the so-called V-value), λ is the optical wavelength, and n_2 is the refractive index of the cladding. We chose $V = 2.1$ at the laser diode wavelength of 0.85 μm for all fibers in the cabling experiment. Fiber parameters may be changed according to Eq. (1). The relative index difference Δ was chosen between 0.1 % and 0.3 % to determine the influence of the Δ-value on loss increases. The core diameters are about 5 μm to 9 μm for the

Δ-value range. The designed fibers have a cutoff wavelength of λ_c = 0.74 μm. The core diameters of GeO_2-doped silica fibers were determined from the interferograms of the sliced preforms. The core diameter in the preform was measured as well as the outer diameter of the preform. The outer diameter of the resulting fiber was then measured after drawing, so that the fiber core diameter is given by the product of the preform core diameter and the preform/fiber outer diameter ratio. Since the index profile of the core is somewhat graded, the width having a half value of the maximum refractive index was adopted as the core diameter [5].

The V-value of the fiber was measured by the wavelength dependence of loss increases caused by fiber bending [6]. The length of the measurement fiber was not more than 50 cm to avoid cutoff wavelength shift to the shorter wavelengths due to the attenuation of the higher modes [7] in a long fiber. The relative index difference was calculated by Eq. (1) together with the measured values of core radius a and the V-value, assuming the refractive index to be a perfect step profile.

The outer diameter of the fiber is 150 μm; each fiber has a primary coating several micrometers thick.

2.2 Coated fiber structure

Figure 1 (a) shows the coated fiber structure. The fibers were coated by nylon with a silicone-buffer layer. This structure is stable against various environmental attacks [8], such as lateral force and low temperatures. The outer diameters of the nylon coating and the silicone-buffer layer are 0.7 mm and 0.4 mm, respectively.

2.3 Cable structure

The cross section of the cable structure is shown in Fig. 1 (b). The central strength member and laminated aluminum polyethylene sheath (LAP sheath) were used for greater mechanical strength. Coated fibers were stranded around a strength member having a 1.5-mm outer diameter. Core wrap was used to protect the stranded fibers from external force.

Coated fibers are usually stranded, because local stresses of the fibers are reduced when the cable is bent. However, bending due to stranding causes loss increases. When a coated fiber having radius ρ_2 is stranded around a central strength member having radius ρ_1, bending radius ρ of the coated fiber is given by

$$\rho = \frac{p^2}{4\pi^2(\rho_1+\rho_2)} + \rho_1+\rho_2, \qquad (2)$$

where p is the stranding pitch. The loss increase was evaluated by the bending loss formula for the $LP_{\nu\mu}$ mode [9] and Eq. (2). Bending loss formulas [10] are shown by

$$\alpha_{01} = \frac{\sqrt{\pi}\ \kappa^2\ \exp[-2/3\ (\gamma^3/\beta^2)\rho]}{2\gamma^{3/2}\ V^2\sqrt{\rho}\ K_{-1}(\gamma a)K_1(\gamma a)} \qquad (3)$$

for the LP_{01} mode, and

$$\alpha_{11} = \frac{\sqrt{\pi}\ \kappa^2\ \exp[-2/3\ (\gamma^3/\beta^2)\rho]}{\gamma^{3/2}\ V^2\sqrt{\rho}\ K_0(\gamma a)K_2(\gamma a)} \qquad (4)$$

for the LP_{11} mode, where β is the axial propagation constant, and κ and γ are the transverse propagation constants in the core and cladding, respectively. $J_\nu(z)$ and $K_\nu(z)$ are Bessel and modified Bessel functions, respectively. The loss increase α for a stranded fiber of length L is given by

$$\alpha = -10\ \log[\exp(-\alpha_{01}L)] \qquad (5)$$

$$V < 2.405$$

$$\alpha = 10\ \log \frac{3}{\exp(-\alpha_{01}L) + 2\exp(-\alpha_{11}L)} \qquad (6)$$

$$V \geq 2.405$$

Two modes above cutoff were assumed to be equally excited

at the fiber input. Figure 2 shows stranding loss increases calculated for four relative index differences. It is clearly seen in Fig. 2 that stranding losses decrease by choosing a large stranding pitch. A stranding pitch p=100 mm was selected to prevent loss increases in the cabling experiment.

§3. Experimental Results on the Cabling Loss Increase

A single-mode optical fiber cable of 850-m length was manufactured; loss measurements were made after each step in the process.

Figure 3 shows the setup for measuring optical loss. The optical loss vs wavelength characteristic was measured using an incoherent source and a monochromator. A launching lens with N.A. = 0.1 and a focal length f = 31.5 mm was used. Silicone oil with n = 1.505 was used to remove cladding modes. The optical power output from the fiber cable was detected with a PbS detector operating at dry ice and an ethyl alcohol coolant temperature. The conditions were the same for all measurements throughout the experiment.

3.1 Nylon coating process

The silicone-buffer fibers were coated with nylon

using a 30-mmϕ extruder.

Optical loss changes are shown in Fig. 4, comparing a nylon-coated fiber with a silicone-buffer fiber. Optical loss measurement for a nylon-coated fiber was made within three hours after coating. It is found that no loss increases occur for the V-value region beyond 1.5. However, large loss increases occur for small V-values around 1.2.

Figure 5 shows wavelength dependence of loss increases as a parameter of relative index difference Δ. It is clearly seen that loss increases are large for a small Δ-value fiber. It is concluded, from Fig. 5, that a coated fiber without loss increase can be manufactured for the V-value range between 2 and 2.4 for rather small Δ-value fibers.

The loss reduction in the small V-value region was examined after nylon coating. Experimental results are shown in Fig. 6. The coated fibers were kept at room temperature, which changed about 5 to 20 °C during a day. It is found that the added microbending [11] loss decreases with time after completion of the nylon coating. The loss reduction may be because microbending due to plastic contraction during the cooling process decreases in a plastic relaxation effect. A coated fiber without

loss increase for wide V-value can be manufactured using this effect. A small Δ-value fiber requires a long time to decay to the original loss value. The relaxation time is considered to be several hundred hours, though it may change with different manufacturing conditions and relaxation temperatures.

Relative index difference dependence on loss increase within three hours after coating is shown in Fig. 7. No loss increases were observed for large Δ-value fibers. The limited Δ-value, where no loss increases occur just after coating, can be selected in Fig. 7.

3.2 Cabling process

Optical loss measurements were made on three processes, i.e., stranding, wrapping, and sheathing. Loss increases on each process are shown in Fig. 8. Stranding loss increase, calculated by Eqs. (5) and (6), is also shown in Fig. 8. It is found that a wide V-value region without loss increases was observed. The loss increase near cutoff wavelength λ_c is that of LP_{11} mode. The LP_{01} mode is believed to incur no loss increase in this region. When $\alpha_{01} \to 0$, $\alpha_{11} \to \infty$, and $L = 1$ km in Eq. (6), the loss value is 4.77 dB/km. This value is consiste with the experimental result. Since the loss increase

of the LP_{01} mode in the small V-value region is consistent with theoretical value, this is mainly caused by bending of stranding. The discrepancy of loss increase after sheathing may be due to microbending by fastening the fibers coated by a LAP sheath to avoid fiber dancing.

Relative index difference dependence on loss increases after sheathing are shown in Fig. 9. It is shown in Fig. 9 that small Δ-value fibers indicated large loss increases. Therefore, special attention must be paid when cabling small Δ-value fibers. The limited Δ-value, where no loss increases occur, can be determined from Fig. 9.

§4. Suitable Fiber Parameters

When constructing single-mode fiber cable transmission systems, loss increases occur from both cabling and splicing. Both loss increases depend on fiber parameters. Since the cabling loss is essentially due to fiber bending, it can be reduced by selecting a large relative index difference Δ. Splicing loss, on the other hand, can be reduced by large core radius a. Therefore, suitable parameters are determinable by minimizing cabling and splicing losses.

4.1 Splicing loss

Splicing losses are mainly caused by transverse and angular displacements. Simple formulas for splicing losses have been derived for small transverse displacement x. Splicing loss α_s is denoted [12] by

$$\alpha_s \simeq 4.34\ K_x\ (x/a)^2, \qquad (7)$$

where

$$K_x = \left[\frac{\gamma a\ J_0(\kappa a)}{J_1(\kappa a)} \right]^2/2. \qquad (8)$$

It is believed that the arc fusion method is suitable, because high reliability is required for single-mode fiber splicing. Recently, low-loss splices by this method have been reported [13]. The average splicing losses of 0.4 dB, 0.2 dB, and 0.1 dB for the fibers with 5.2-μm, 7-μm, and 10-μm core diameters, respectively, are obtained at a V-value of 2.4. The average transverse displacements of the fibers spliced by the apparatus were calculated with Eq. (7) and the splicing losses. The calculated values were about 0.9 μm for the three fibers. Therefore, the splicing loss formula Eq. (7), with an average displacement x = 0.9 μm, can be used to evaluate practical splices.

4.2 Selection method

We have three parameters: relative index difference Δ, core radius a, and the V-value. If any two parameters are determined, the other can be calculated by Eq. (1). We chose the V-value instead of a because it is related to the single-mode condition.

The single-mode condition is denoted by $V < 2.405$ for a step-index fiber. Any value can be selected in the condition, but a large V-value is appropriate because of its strong optical power confinement. In practical use, relative index difference Δ and core radius a have small deviations $d\Delta$ and da from the designed value. The V-value deviation can be estimated by differentiating Eq. (1) and is given by

$$| dV/V | \leqslant | da/a | + \frac{1}{2} | d\Delta/\Delta |. \qquad (9)$$

The safety value V_s of normalized frequency is determined by subtracting dV from the cutoff value V_c, that is, $V_s = 2.405 - dV$. Fiber deviations have been attained within ± 5 % [14] for the both parameters. If the permitted limit is within 7 %, including a little safety margin, the V-value deviation is $dV \simeq 0.25$. The safety value V_s, therefore, is $V_s = 2.2$.

A suitable refractive index difference is determinable

from minimizing the loss increase. The loss increase, added to cabling and splicing losses, is shown in Fig. 10. The cabling and splicing loss increases are shown with dotted lines. Cabling loss increases were already shown in Fig. 9, and only the loss increase curves smaller than 3 dB/km are drawn in Fig 10. The splicing loss was calculated by Eq. (7), assuming that splices are located one kilometer apart. When the safety V-value V_s is designed, it must deviate $V_s \pm dV$. For safe use, the refractive index difference Δ should be determined in correspondence with $V_s - dV$. Therefore, the Δ-value is selected by the loss minimum point for $V = 1.9$ curve in Fig. 10. The selected value is $\Delta = 0.2$ %.

Recently, low-loss single-mode fibers in the 1.1 - 1.6 μm wavelength region were fabricated [15], and the optical loss was smaller than 1 dB/km. The selection method we discussed here is also applicable to low-loss fibers in the 1.1 - 1.6 μm wavelength region, though it was discovered in using the fibers designed in the wavelength region around 0.85 μm.

§5. Conclusion

We made an eight single-mode fiber cable and shown the existence of a wide V-value region without cabling loss

increases. The cable structure is a simple strand-type consisting of separately coated fibers. The manufactured cable has a small diameter, is light weight, and is expected to be stable against various environmental attacks through a suitable arrangement of buffer material. In the fiber coating process, microbending loss reduction was observed. Coated fibers without a loss increase can be manufactured by using this effect for rather small Δ-value fibers.

A new method has been described for determining suitable fiber parameters to construct a low-loss transmission system. Suitable fiber parameters are determinable by minimizing cabling and splicing loss increases. Suitable values are $\Delta = 0.2\ \%$ and $V = 2.2$ when using this method.

References

1. A. Kawana, T. Miyashita, M. Nakahara, M. Kawachi, and T. Hosaka: 'Fabrication of low-loss single-mode fibres', Electron. Lett., 13, 7, p.188 (1977)
2. D. Gloge: 'Optical-fiber packaging and its influence on fiber straightness and loss', Bell Syst. Tech. J., 54, 2, p.245 (1975)
3. T. Kobayashi, Y. Sugawara, R. Yamauchi, K. Inada and N. Uchida: 'Stress in fibers during optical cable manufacturing process and installation', Proceedings of the Twenty-Seventh International Wire and Cable Symposium, p.362 (1978)
4. G. W. Tasker, W. G. French, J. R. Simpson, P. Kaiser, and H. M. Presby: 'Low-loss single-mode fibers with different B_2O_3-SiO_2 compositions', Appl. Opt., 17, 11, p.1836 (1978)
5. T. Miyashita, A. Kawana, M. Nakahara, M. Kawachi and T. Hosaka: 'Fabrication of GeO_2 doped silica single-mode fiber', Trans. IECE of Japan, E-61, 11, p.891 (1978)
6. Y. Katsuyama, M. Tokuda, N. Uchida and M. Nakahara: 'New method for measuring V-value of a single-mode optical fibre', Electron. Lett., 12, 25, p.669 (1976)
7. W. A. Gamblig, D. N. Payne, H. Matsumura and S. R. Norman: 'Measurement of normalised frequency in single-

mode optical fibres', Electron. Lett., 13, 5, p.133 (1977)

8. T. Naruse, Y. Sugawara, and K. Masuno: 'Nylon-jacketed optical fibre with silicone buffer layer', Electron. Lett., 13, 6, p.153 (1977)
9. D. Gloge: 'Weakly guiding fibers', Appl. Opt., 10, 10, p.2252 (1971)
10. D. Marcuse: 'Curvature loss formula for optical fibers', J. Opt. Soc. Am., 66, 31, p.216 (1976)
11. W. B. Gardner: 'Microbending loss in optical fibers', Bell Syst. Tech. J., 54, 2, p.457 (1975)
12. Y. Murakami, I. Hatakeyama, and H. Tsuchiya: 'Normalised frequency dependence of splice losses in single-mode optical fibres', Electron. Lett., 14, 9, p.277 (1978)
13. I. Hatakeyama and H. Tsuchiya: 'Fusion splices for single-mode optical fibers', IEEE J. Quantum Electron., QE-14, 8, p.614 (1978)
14. T. Miya, Y. Terunuma, T. Hosaka, and T. Miyashita: 'Ultra low loss single-mode fibers at 1.55 μm', Rev. Electr. Commun. Lab. NTT Jpn., 27, 7-8, p.497 (1979)
15. M. Kawachi, A. Kawana, and T. Miyashita: 'Low-loss single-mode fibre at the material-dispersion-free wavelength of 1.27 μm', Electron. Lett., 13, 15, p.442 (1977)

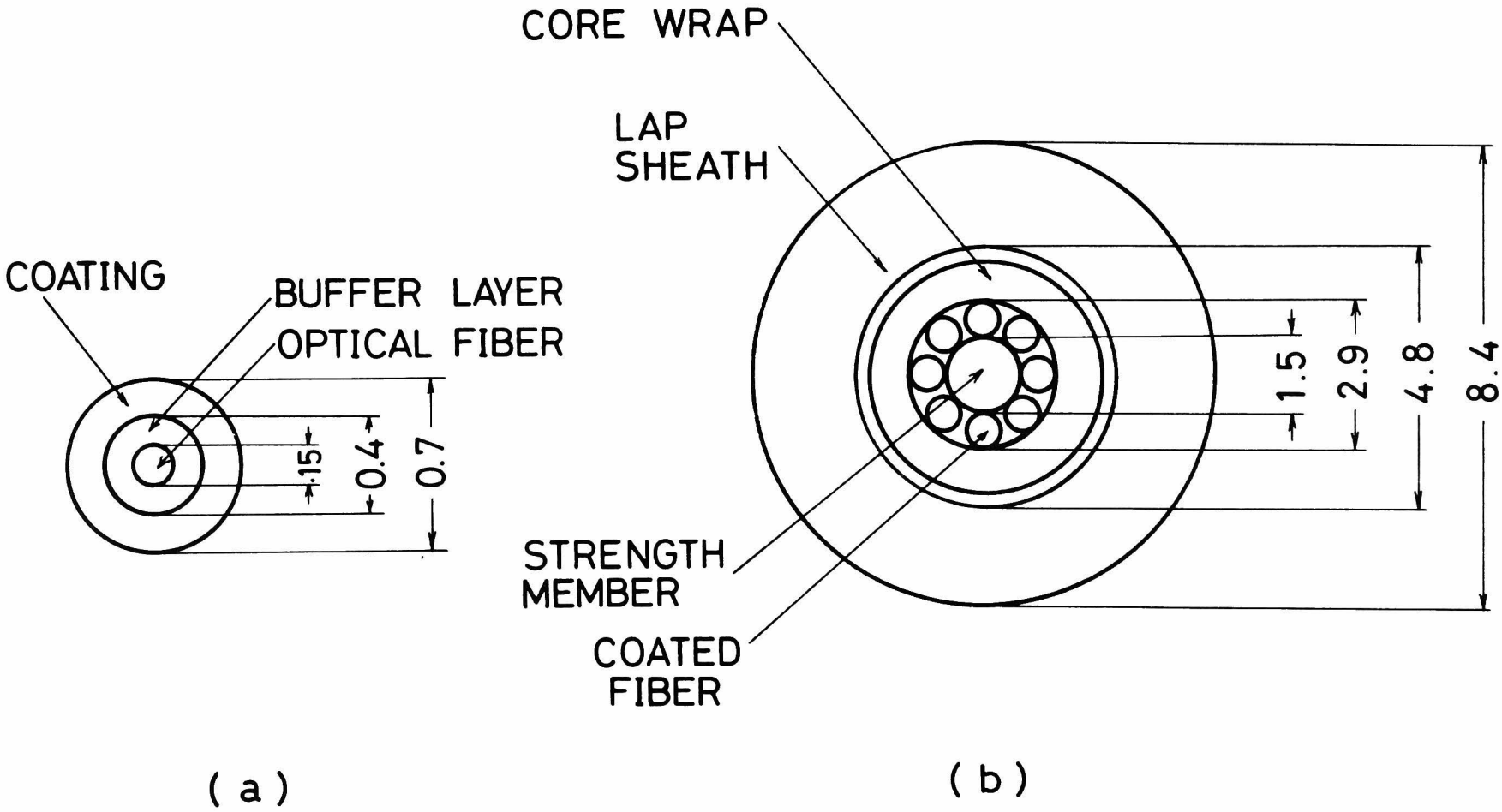

Fig. 1 Coated fiber structure and cable structure.

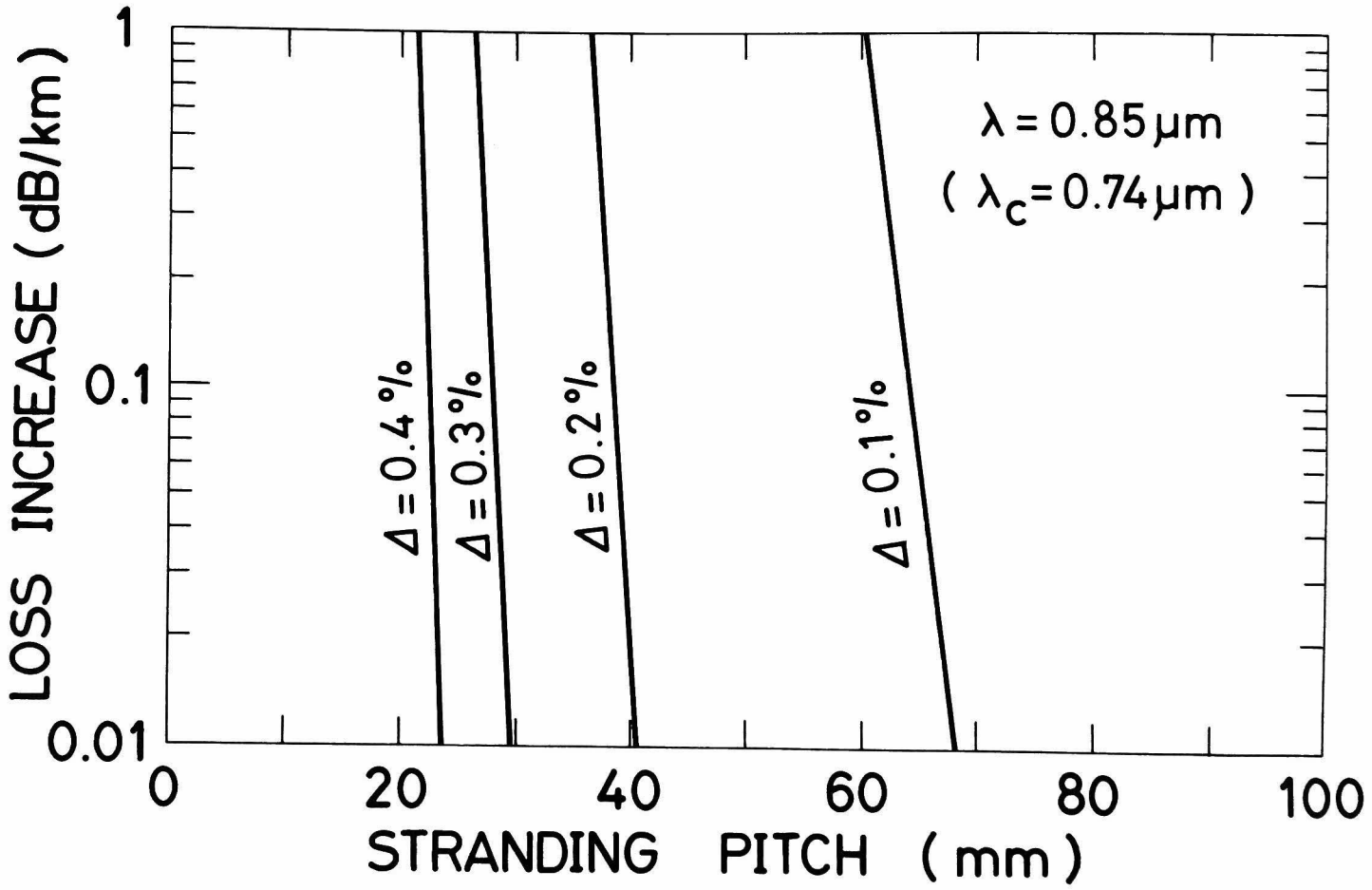

Fig. 2 Calculated loss increase for coated fiber due to stranding.

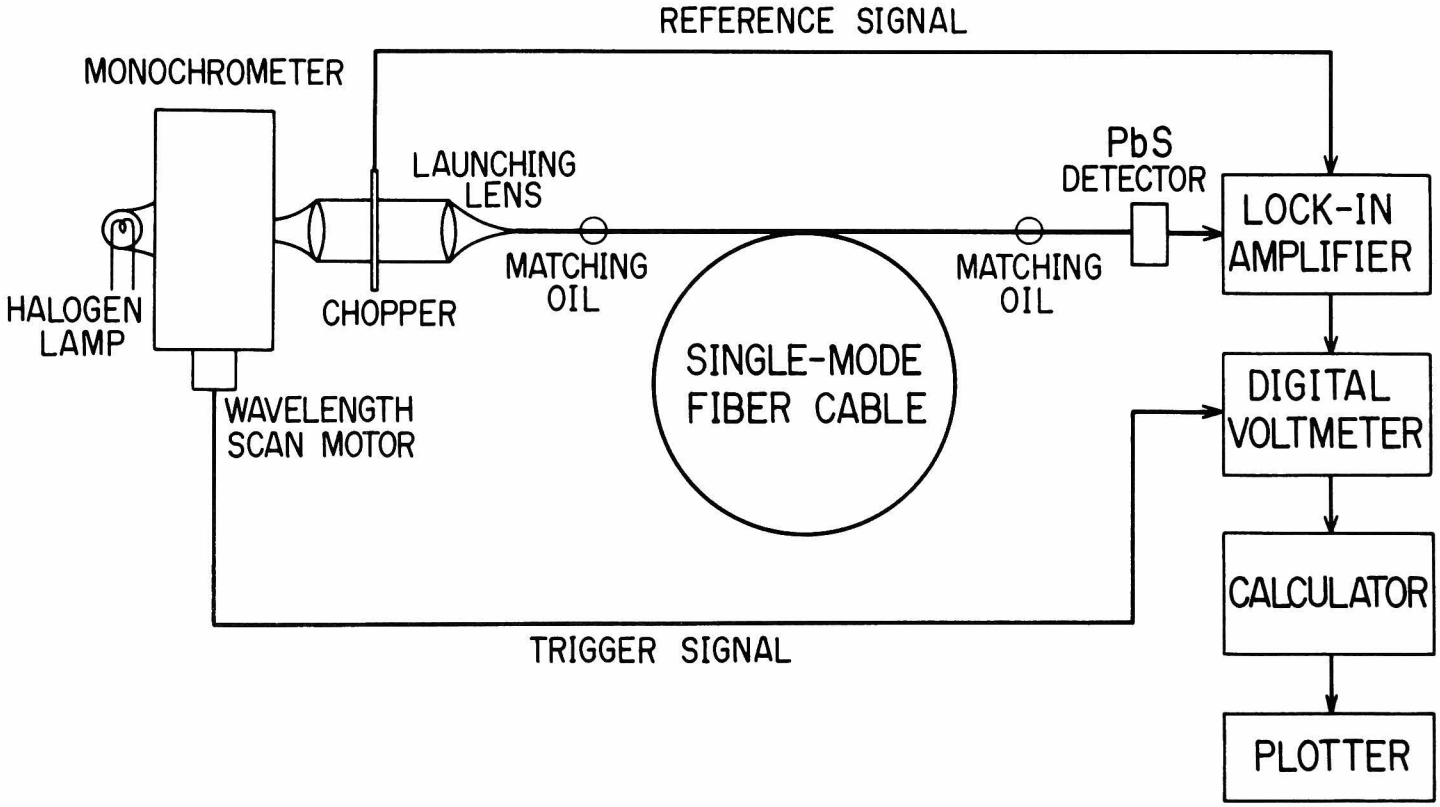

Fig. 3 Setup for measuring optical loss.

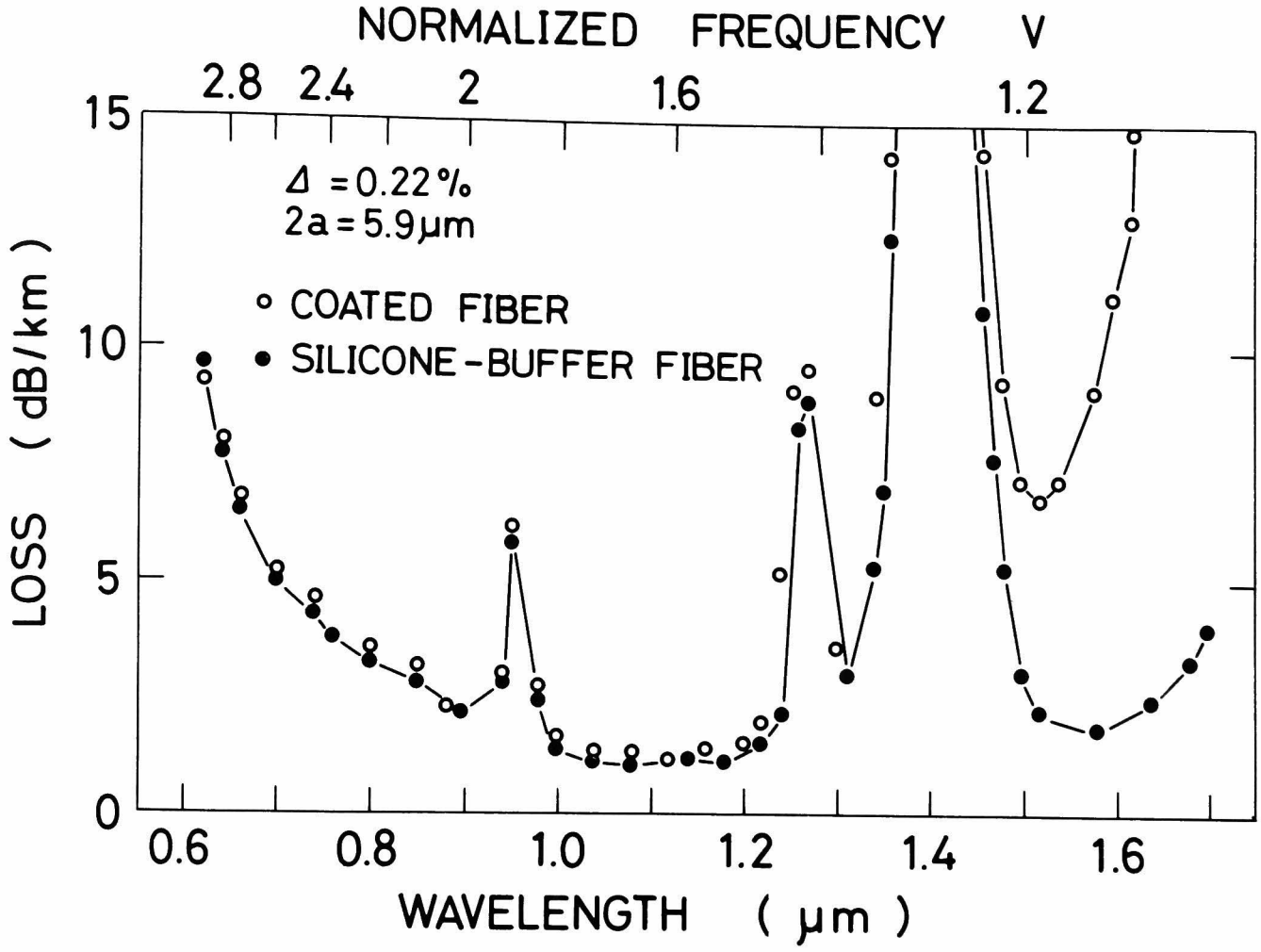

Fig. 4 Optical loss changes due to nylon coating. Loss measurement for coated fiber was made within 3 hours after coating.

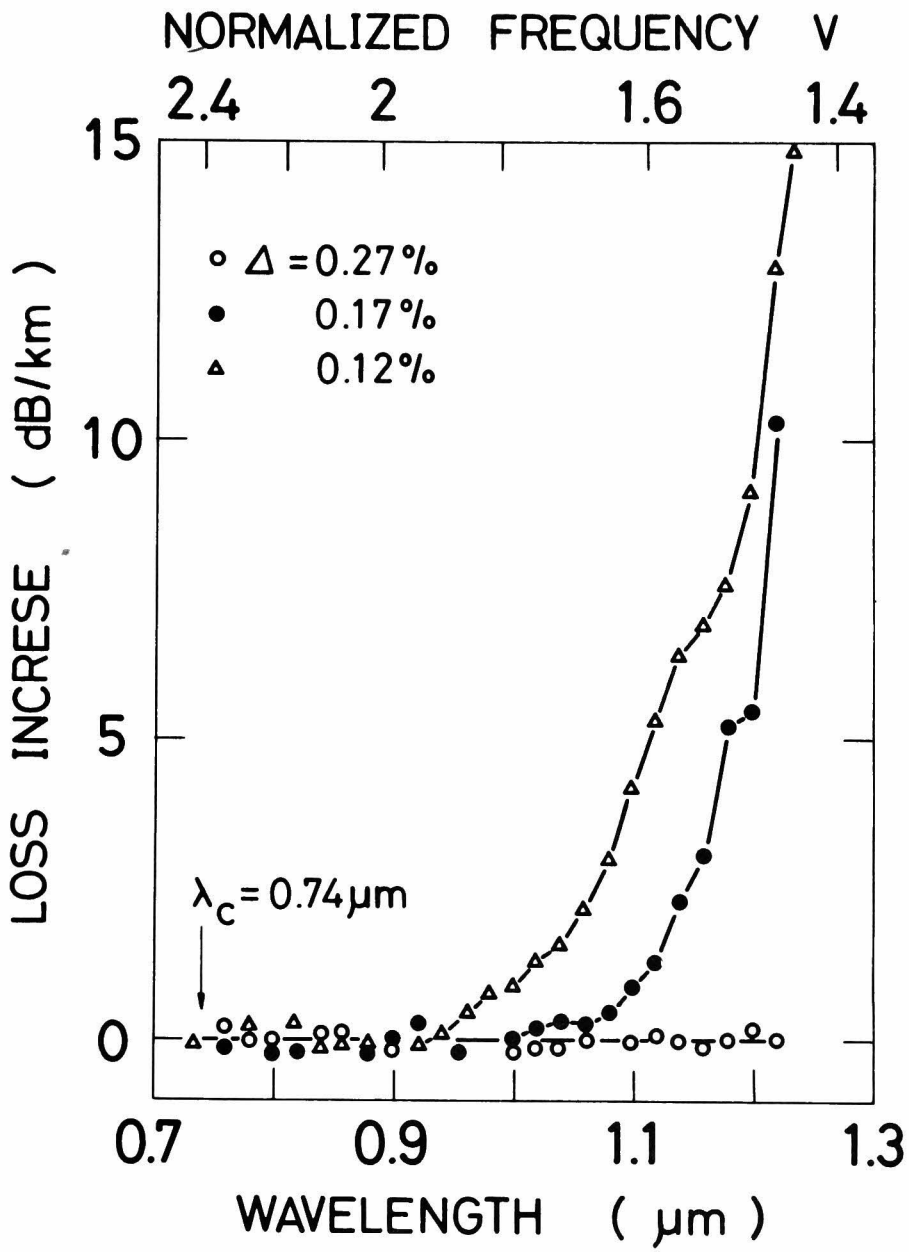

Fig. 5 Wavelength dependence of loss increase due to coating. Loss measurements were made within 3 hours after coating.

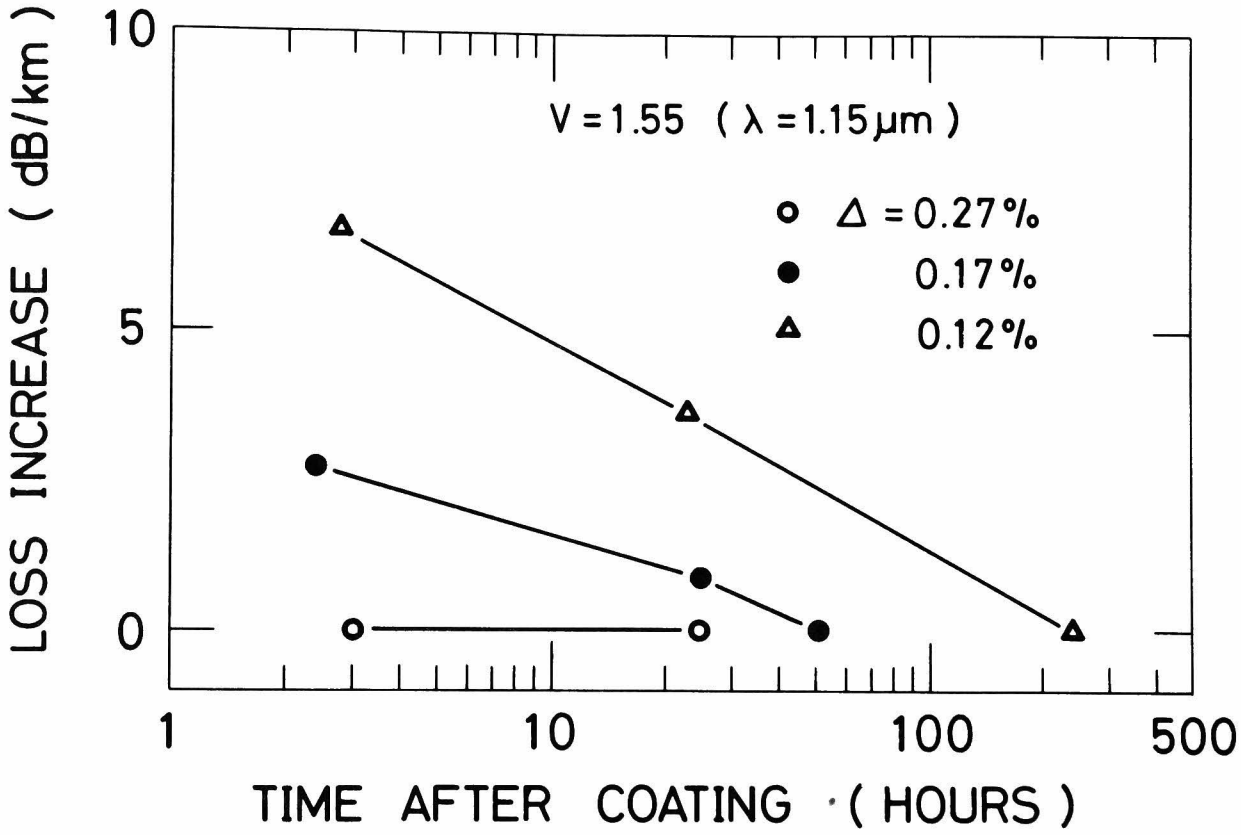

Fig. 6 Loss increases due to coating decrease with time.

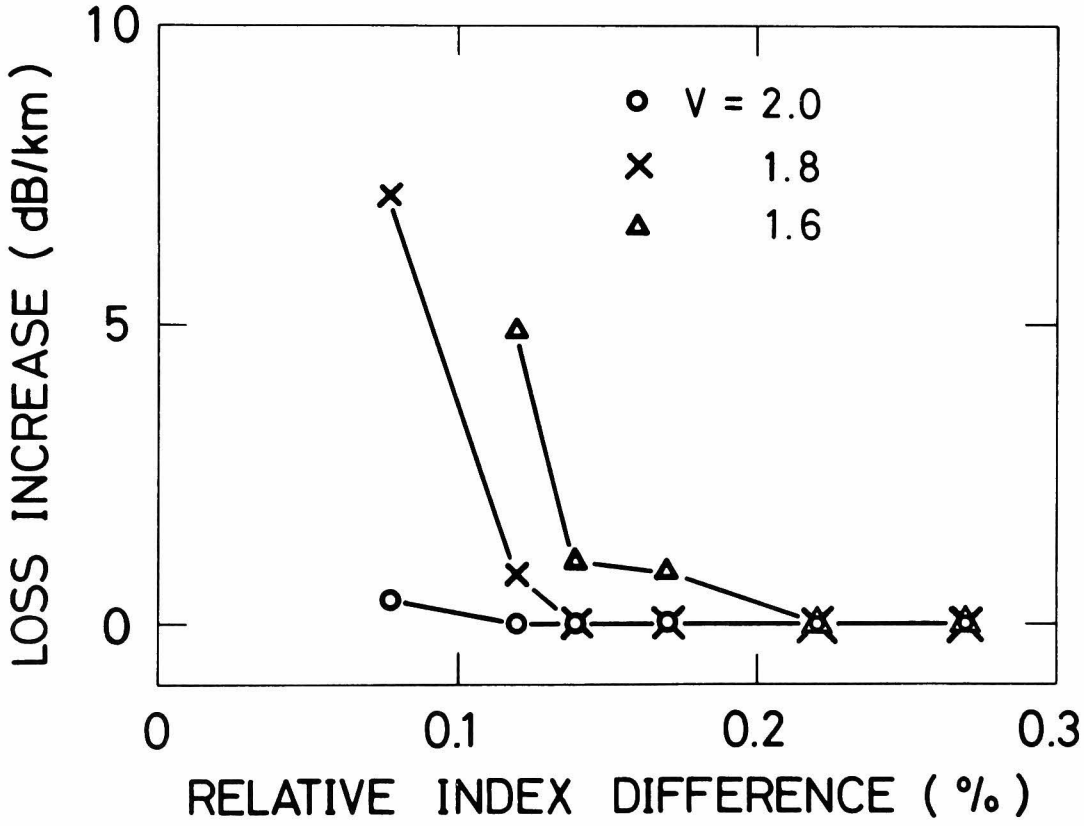

Fig. 7 Relative index difference dependence of loss increases within 3 hours after coating.

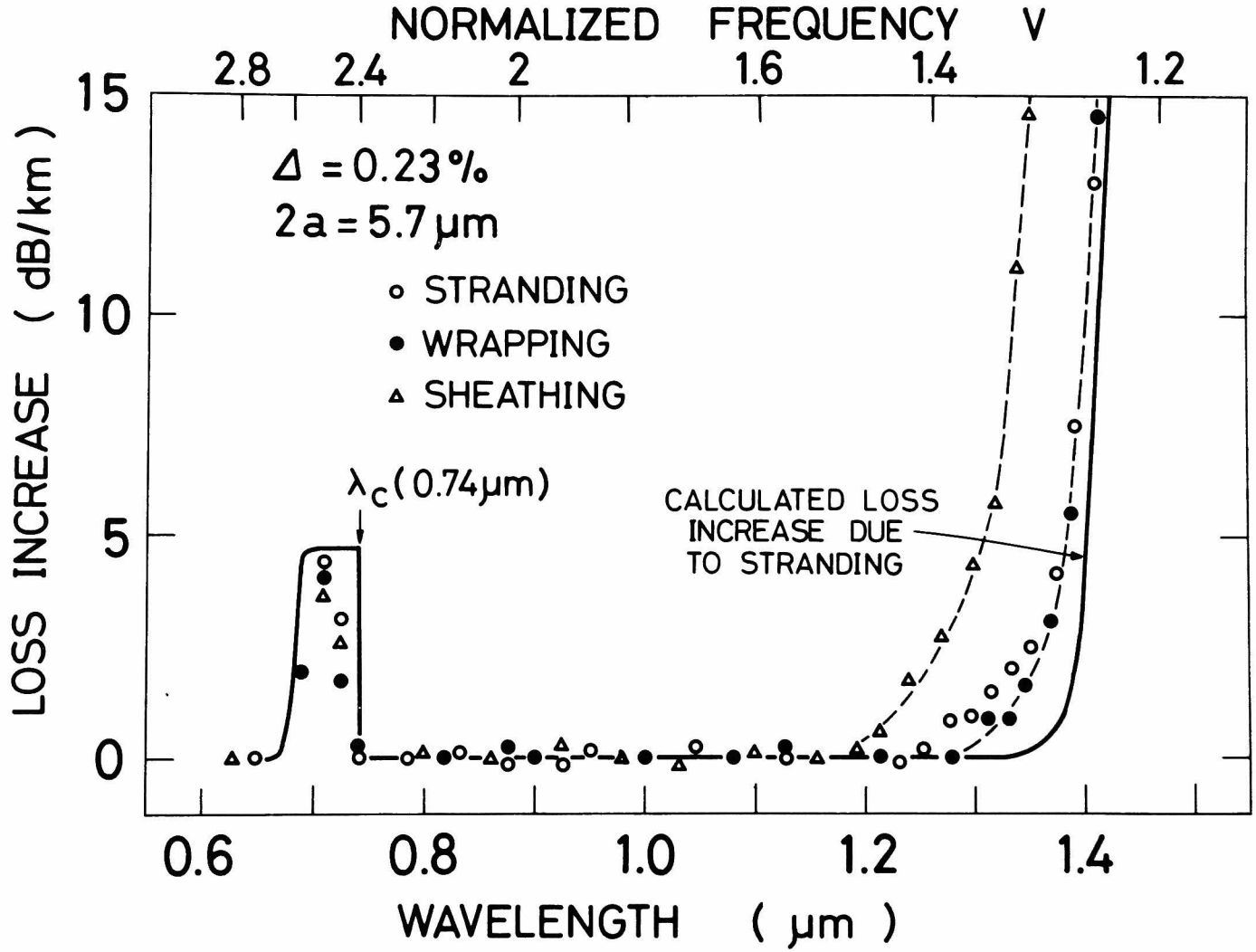

Fig. 8 Loss increase characteristics in each cabling process.

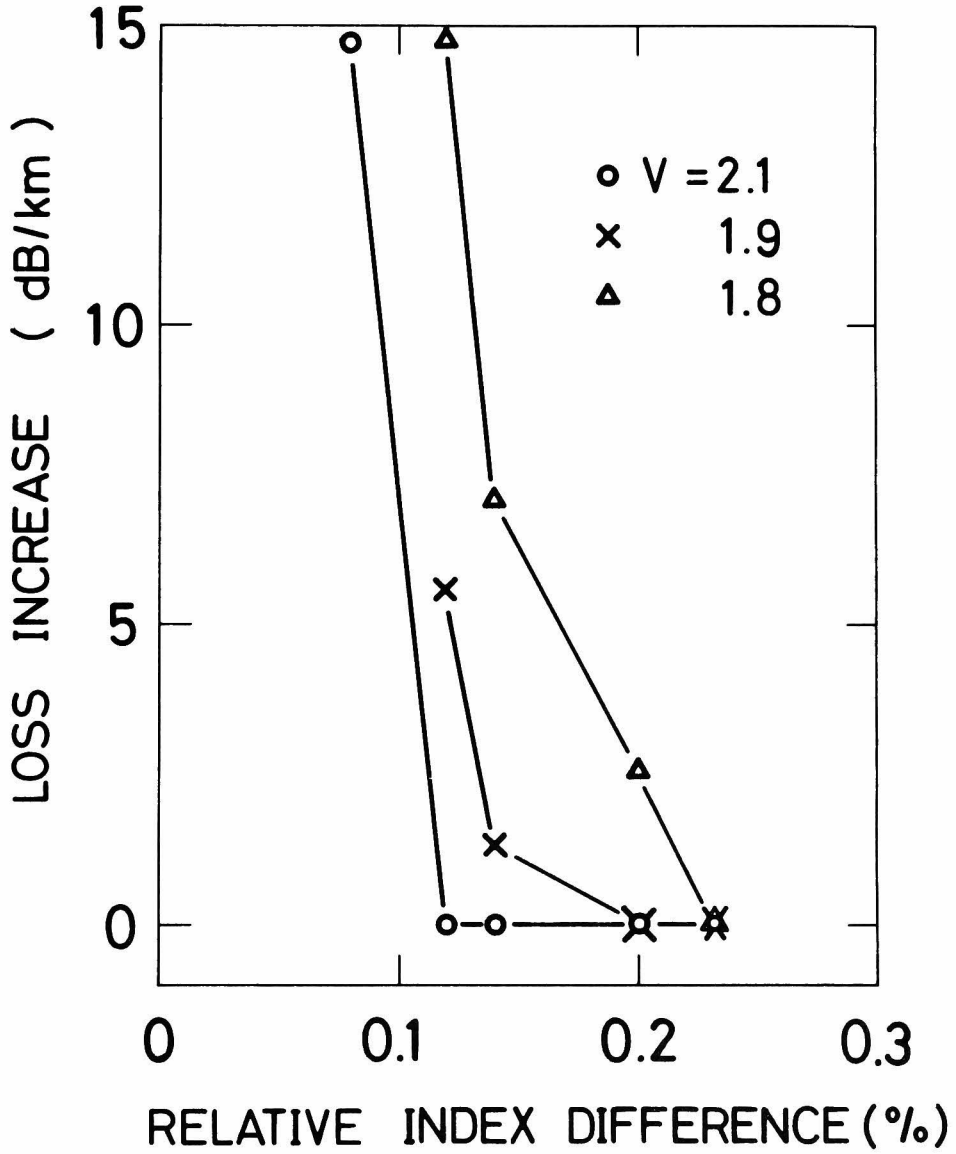

Fig. 9 Relative index difference dependence of loss increases due to cabling.

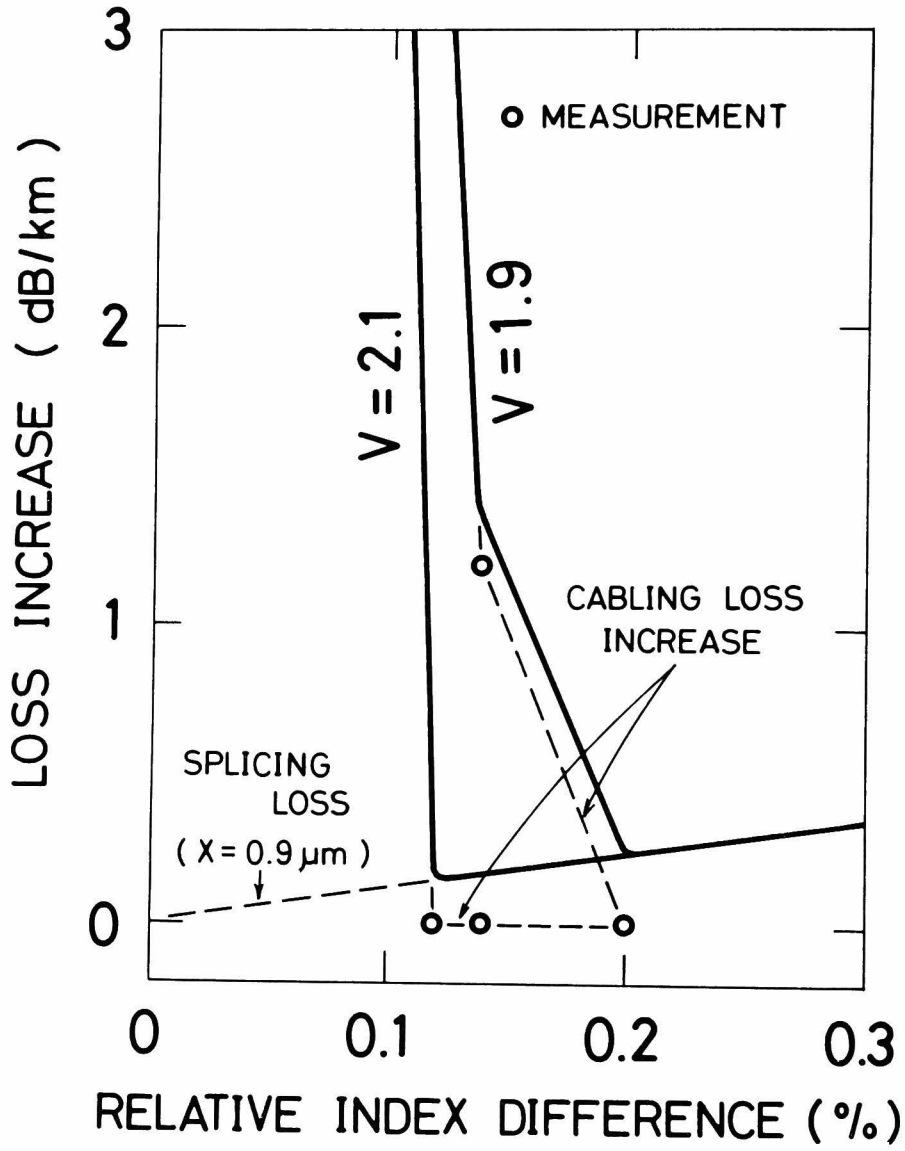

Fig. 10 Relative index difference minimizing cabling and splicing losses.

CHAPTER III STRAIN MEASUREMENT IN OPTICAL FIBER CABLE USING RESISTANCE WIRE

Synopsis

Resistance wire method was proposed for measuring longitudinal strain of a glass fiber in an optical cable. In this method, strain is evaluated by measuring the resistance change of a metal wire coated with the same material for a glass fiber. It was confirmed that the resistance change rate $\Delta R/R$ was in proportion to the strain. An optical cable containing both a coated resistance wire and coated fibers was manufactured, and the strain in the cable was measured under tension, bending and vibration. The results are valuable in mechanical design of a fiber cable. Thus, the resistance wire method is found to be simple and useful to evaluate a fiber strain inside an optical cable.

§1. Introduction

Optical fiber is an attractive transmission medium, but it is important to guard against the mechanical failure of the glass fibers, because they are made of brittle material. Furthermore, irregular stresses cause loss increase [1], even if the stress is smaller than the failure value. Therefore, many kinds of cable structures have been proposed and evaluated in an effort to develop a highly reliable cable. For example, it was reported [2] that appropriate arrangements of cushion material soften the external forces and that the inclusion of a strength member provides the cable with enough mechanical strength.

Accurate evaluation of the fiber strain is required in the mechanical design. However, it is difficult to measure the fiber strain in the cable under various external forces. Recently, the fiber strain in a cable subjected to a tensile load has been measured by a pulse method [3], which consists of measuring the pulse delay time change due to fiber elongation. This method is useful because an optical pulse passing through the elongated fiber is measured directly. However, a long fiber must be used in order to make accurate measurements because of the small change in delay time. The pulse method is not suitable for ordinary mechanical test using

short cable pieces.

We propose resistance wire method to evaluate fiber strain, which is given by measuring the resistance change of a metal wire. The resistance wire was coated with the same plastic material as that for optical fiber, and then optical cable was manufactured containing a coated wire instead of ordinary coated fibers. Strain measurements were made for the optical cable under some kinds of external force. In this chapter, fundamental strain characteristics of the coated wire are presented, and measured strains inside the cable under several external forces are described.

§2. Coated Resistance Wire

2.1 Relation between strain and resistance change

Many studies on resistance change due to strain were reported in relation to strain gauge [4]. In this section, an outline is described.

When a resistance wire having length L, cross-sectional area A and specific resistance ρ is elongated by ΔL, the resistance change ΔR is given by

$$\Delta R/R = (1+C)\Delta L/L - (1-C)\Delta A/A, \qquad (1)$$

where R is the original resistance, ΔA is cross-sectional area change and C is a constant related to the wire

material. It is apparant from Eq. (1) that resistance change is caused by elongation ΔL and cross-sectional area change ΔA.

Resistance change under several cases of external force is expressed as follows. We assumed that wire elongation is within the elastic limit, considering the fact that fiber strain in a cable is usually small.

First, in case of tensile load, the following experessions hold.

$$\left.\begin{aligned} \Delta L/L &= \varepsilon_z, \\ \Delta A/A &= \varepsilon_r + \varepsilon_\theta = -2\nu\varepsilon_z, \end{aligned}\right\} \qquad (2)$$

where ε_z, ε_r and ε_θ are longitudinal, radial and circumferential strain, respectively, and ν is Poisson's ratio. Substitution of Eq. (2) into Eq. (1) leads to

$$\Delta R/R = K\varepsilon_z, \qquad (3)$$

where

$$K = 1 + 2\nu + (1-2\nu)\, C. \qquad (4)$$

The constant K is called as gauge factor for ordinary strain gauge. When K value of the wire is determined, longitudinal strain ε_z can be evaluated by measuring the resistance change.

Second, in case of bending and tortional force, total changes of L and A are zero. Therefore, no resistance changes occur, according to Eq. (1).

2.2 Fundamental strain characteristics of coated resistance wire

Copper-nickel alloy was adopted for the resistance wire material. The physical properties are listed in Table I. Coated wire structure is shown in Fig. 1. The resistance wire with silicone buffer layer was coated with nylon. This structure is the same as the three-layer structure [5] for optical fiber.

The bridge circuit shown in Fig. 2 was used to measure resistance change. The resistance value R in the bridge circuit is variable in the range of 120 Ω to 60 kΩ. These values are equal to the wire resistances of 4 m to 2 km length, respectively. Measurement error for $\Delta R/R$ was attained within 10^{-6}.

Figure 3 shows the measured relation between resistance change and strain of the coated wire. The coated wire was elongated with a tensile test machine and the resistance change was measured during the test process. It is found that the resistance change rate $\Delta R/R$ is in proportion to the strain. The proportionality constant

K is given by

$$K = 2.18 \qquad (5)$$

from Fig. 3. Calculation of C using K and ν according to Eq. (4) leads to

$$C = 1.45. \qquad (6)$$

Figure 4 shows the relation between tensile load and strain for resistance wire, coated resistance wire and nylon string. The diameter of the nylon string was chosen to be 0.8 mm. The cross-sectional area of the string was equal to the nylon area of the coated resistance wire. It is found that the tensile load for the resistance wire is proportional to the strain. The Young's modulus evaluated from Fig. 4 is 15000 kg/mm^2 as listed in Table I. However, the tensile load is not proportional in the strain region larger than 0.2 %. In this region, Equation (2) does not hold, and measurement error becomes large. Therefore, we restricted the measurement to the smaller strain region than 0.2 % in this method. The tensile load for the coated resistance wire is found to be larger than that for the bare resistance wire at the same strain value. This is due to the nylon coating. The tensile load for the coated wire is equal to the sum of the measured loads for wire and nylon at

each strain.

Resistance change measurements were made for a coated wire due to bend and torsion. However, no changes were observed within the measurable limit. This is consistent with the consideration given in §2.1. It is concluded that the longitudinal strain can be evaluated correctly by measuring the resistance change.

§3. Fiber Strain Measurement in Optical Cable

An optical cable was manufactured which contained both a coated resistance wire and coated fibers. Cross section of fiber unit is shown in Fig. 5. The resistance wire was coated and stranded to construct the fiber unit in the same way as other optical fibers were. The optical fibers are made of fused silica and the diameter is 0.125 mm. Figure 6 shows cross section of the optical cable. This cable contains a central steel strength member, ten interstitial quads and four fiber units. The fiber units were stranded around the strength member with a pitch of 600 mm. Since the optical cable consists of many kinds of material as shown in Fig. 6, fiber strain in the cable subjected to external force is very complicated. In resistance wire method, wire elongation can be measured simply. As for the fiber elongation, the rigidity of

the silica fiber is different from that of the resistance wire and a correction may be necessary. However, in case of ordinary optical cable, almost all mechanical characteristics are determined by the metal materials. This is because the total rigidity of the metal materials is much larger than that of the resistance wires. Therefore, it is considered that no essential difference occurs between the strains of optical fiber and resistance wire in the cable.

3.1 Tensile load

The optical cable was elongated with a tensile test machine. A gauge length of 0.5 m was chosen in a cable piece of 0.7 m. The cable sheath of 0.1 m long was teared at the both ends, and all the materials were fixed with epoxy resin. Tensile test was made by pulling down the fixed ends. The coated wire was taken from the fixed ends, and the resistance change was measured during the test process. In Fig. 7, measured strain by the resistance wire and a strain gauge put on the cable sheath are shown by circles. The strain measurements were also made for the strength member only (St. M.) and the composite of strength member and ten interstitial quads (St. M. + Int. Quads). The results are shown by broken and solid

lines, respectively. It is found that the measured results by the resistance wire and strain gauge agree well with each other. Furthermore, the values are consistent with the strain curve for the composite metal materials. This result shows that the elongations of all the parts in the cable are nearly equal to each other, because all the materials were fixed with epoxy resin.

3.2 Bending

When a cable is bent, tension and compression sides appear in the cable. However, it is difficult to estimate the strain because the coated fibers are stranded. Strain measurements were made by changing the bent position relative to the resistance wire. Figure 8 shows measured result. All the materials were fixed with epoxy resin at the cable ends. The cable length of 0.3 m was chosen for bending part. The length is equal to a half of the fiber unit stranding pitch. It is clearly seen that tension and compression strains are measured, and that the maximum and minimum values occur at opposite positions giving a cable bend. This result is consistent with the fact that cable bend causes tension and compresson sides. The absolute values of strain at opposite positions are nearly the same, which indicates that little slip

between the coated wire and the unit strength member occurred during cable bends.

3.3 Vibration

It is expected that an optical fiber cable can be used as an aerial line, because fiber has great capacity applicable to various environments. However, cable stability is unclear under hard vibrations due to wind. We examined, therefore, vibration characteristics of the optical cable.

Figure 9 shows an outline of vibration experiment. An optical cable and a steel messenger wire were aerially installed, and lashing wire [6] fixed them. Only the messenger wire was fixed at the both ends. The variable ranges of vibration amplitude and frequency are 0 to ± 150 mm and 0.01 to 3 Hz, respectively. The optical cable was vibrated at a forth position of the 35 m cable span. The center position of vibration was located on a horizontal line between the both fixed ends.

Figure 10 shows time dependence of fiber strain. It is clearly seen that the strain changes periodically. The periodic time of measured strain is exactly equal to that of the cable vibration. Both cable installation and vibration cause strain, and the measured values are

additional strain due to vibration. Constant value at the bottom of the periodic strain is found as shown in Fig. 10 (a). This is due to cable slack caused by the weight of cable and messenger wire themselves after the cable was installed. Strain increases and then decreases when the cable vibrates upward and downward, respectively. The strain remains constant for a time that the cable vibrates during the slack. However, other small strain peaks appear among large peaks with increasing vibration amplitude as shown in Fig. 10 (b). This small strain peak is due to downward vibration beyond the cable slack. Strain rate must be considered [7] as well as the maximum strain value in preventing fiber failure due to fatigue. The measured result shown in Fig. 10 (b) indicates that the frequency of fiber strain is able to become double value of vibration frequency.

Figure 11 shows vibration frequency dependence of fiber strain. A resonance frequency ν_r for aerially installed cable is given by

$$\nu_r = \frac{n}{2L}\sqrt{\frac{gT}{w}}, \qquad (7)$$

where n, L, g, T and w are mode number, cable span length, gravitational acceleration, cable tension and linear

density, respectively. Substitution of the values $n = 2$, $L = 35$ m, $T = 250$ kg, $w = (0.71 + 0.23)$ kg/m (linear density of cable and messenger wire assembly) leads to

$$\nu_r = 1.5 \text{ Hz}. \qquad (8)$$

Figure 11 shows the experimental result showing that vibration with a resonance frequency causes the maximum strain.

Vibration amplitude dependence of strain was measured to estimate the largest strain when the cable was vibrated with the resonance frequency. The measured results are shown in Fig. 12. It is found that strain increases with larger amplitude. The maximum strain in the vibration conditions is 2.2×10^{-2} %, which is much smaller than the failure value of a silica fiber.

§4. Conclusion

Resistance wire method has been proposed for measuring a longitudinal strain of a glass fiber in an optical cable. Coated resistance wire having the same coating structure for a glass fiber was manufactured and the fundamental strain characteristics have been clarified. Since the resistance change ΔR is in proportion to the strain, correct evaluation of strain can be made by measuring

the resistance change.

An optical fiber cable which contains a coated resistance wire was manufactured. The fiber strain inside the cable was measured under tensile load, bending and vibration. The strain characteristics have been clarified even in a complicated structure of the strand-type optical cable.

In conclusion, resistance wire method is a simple and useful to measure a fiber strain inside a cable. The measured results are useful in mechanical design and evaluation of cable reliability. The measured strain under the external forces are much smaller than the failure strain of silica fiber, which is about a few percent.

References

1. D. Gloge: 'Optical-fiber packaging and its influence on fiber straightness and loss', Bell Syst. Tech. J., 54, 2, p.245 (1975)
2. K. Ishihara, M. Tokuda, and S. Seikai: '48 core optical fiber cable design and characteristics', Rev. Electr. Commun. Lab. NTT Jpn., 27, 11-12, p.949 (1979)
3. T. Kobayashi, Y. Sugawara, R. Yamauchi, K. Inada, and N. Uchida: 'Stress in fibers during optical cable manufacturing process and installation', Proceedings of the Twenty-Seventh International Wire and Cable Symposium, p.362 (1978)
4. For example, Osamu Watanabe: 'Strain Gauge and its Applications', (Nikkankogyo-shinbunsha) [in Japanese]
5. T. Naruse, Y. Sugawara, and K. Masuno: 'Nylon-jacketed optical fibre with silicone buffer layer', Electron. Lett., 13, 6, p.153 (1977)
6. NTT: 'Design Engineers' Handbook' (1975) [in Japanese]
7. R. J. Charles: 'Dynamic fatigue of glass', J. Appl. Phys., 29, 11, p.1657 (1958)

Table I. Physical properties of resistance wire.

Composition	45% Ni - 55% Cu
Young's modulus (kg/mm^2)	15000
Poissoin's ratio ν	0.33
Elastic limit of strain (%)	0.2
Specific resistance ρ (Ω.cm)	5.05×10^{-5}
Coefficient of linear expansion (1/°C)	3.5×10^{-6}
Diameter (mm)	0.15

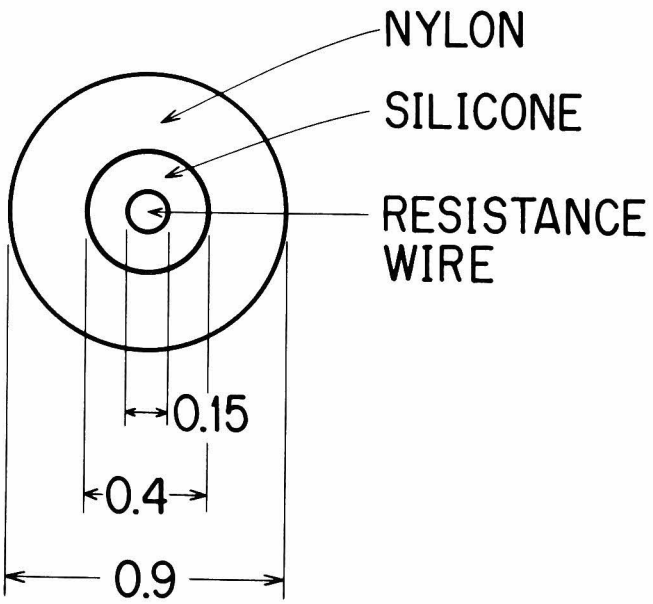

Fig. 1 Coated resistance wire structure.

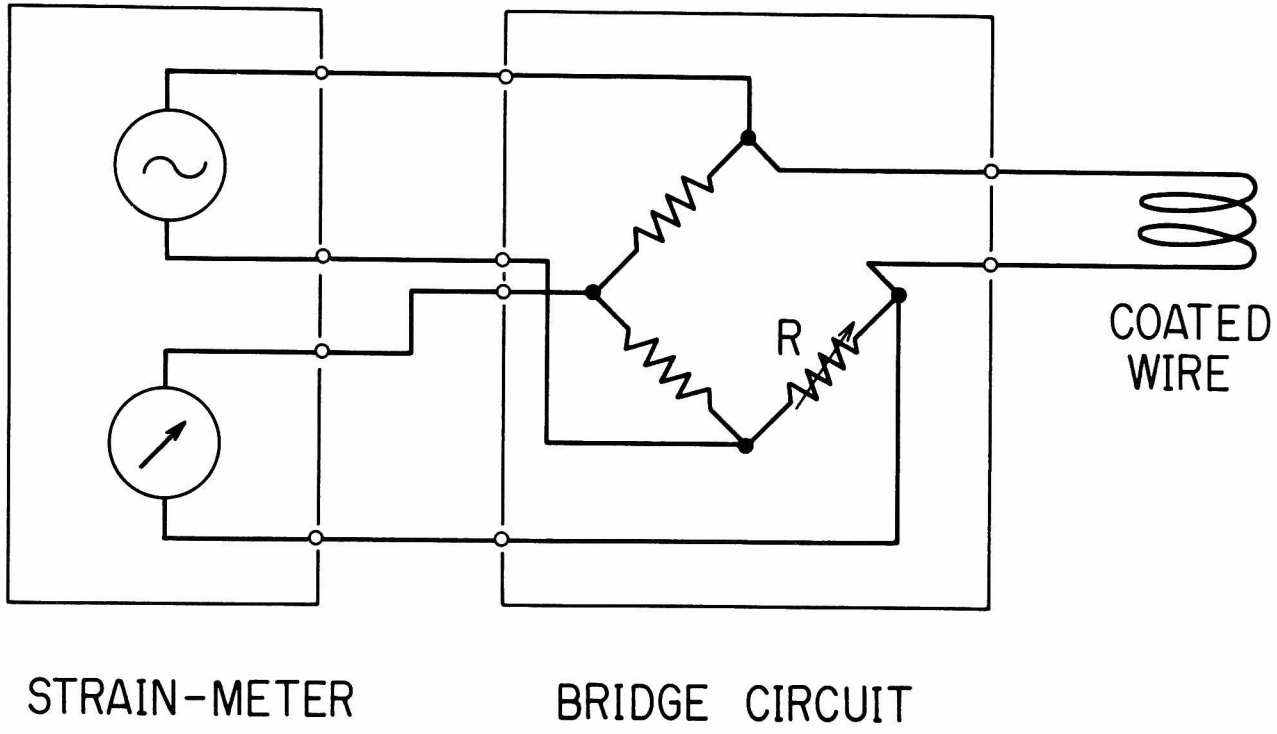

Fig. 2 Setup for measuring resistance change. The resistance R in the bridge circuit is variable, so as to be equal to the value for the coated wire.

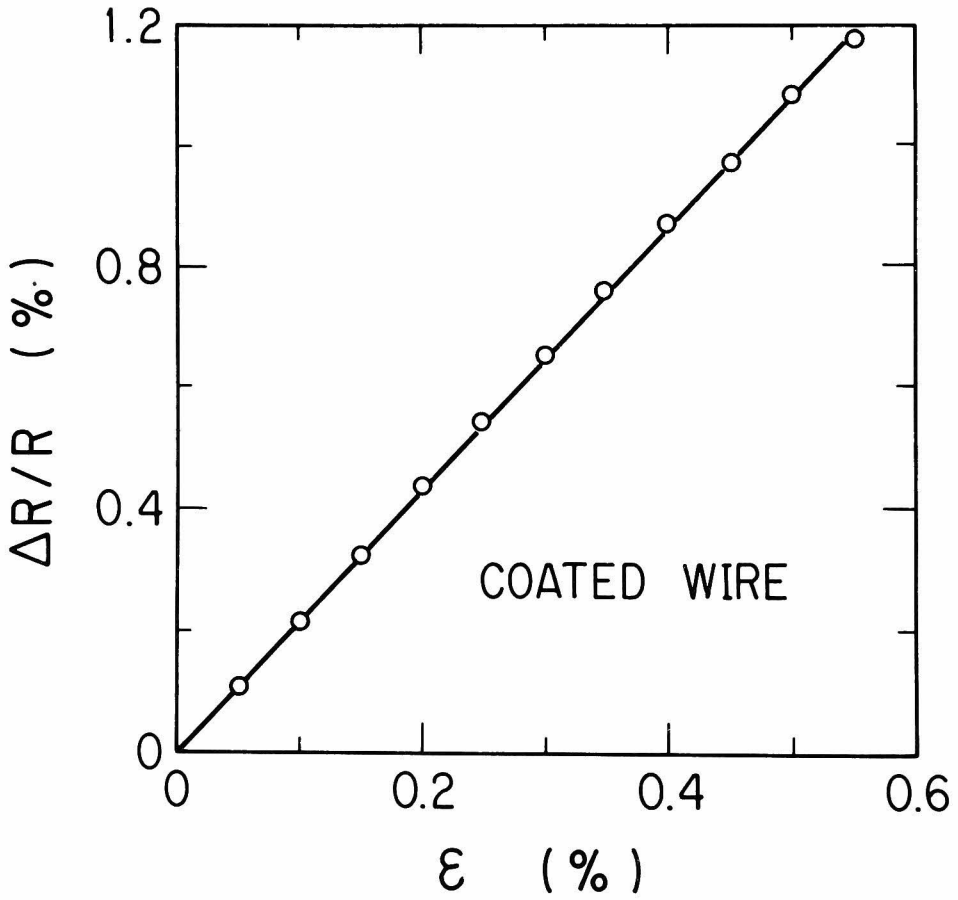

Fig. 3 Relation between resistance change rate ΔR/R and strain ε.

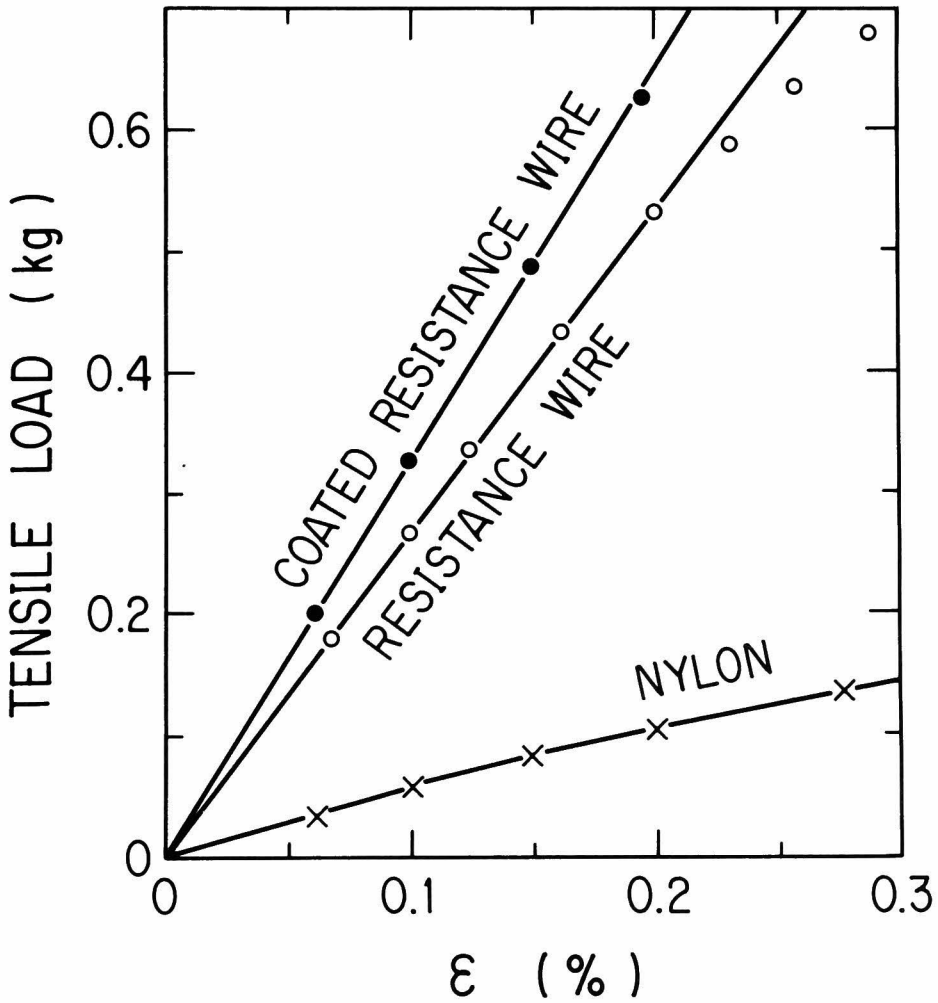

Fig. 4 Measured strain with a tensile test machine.

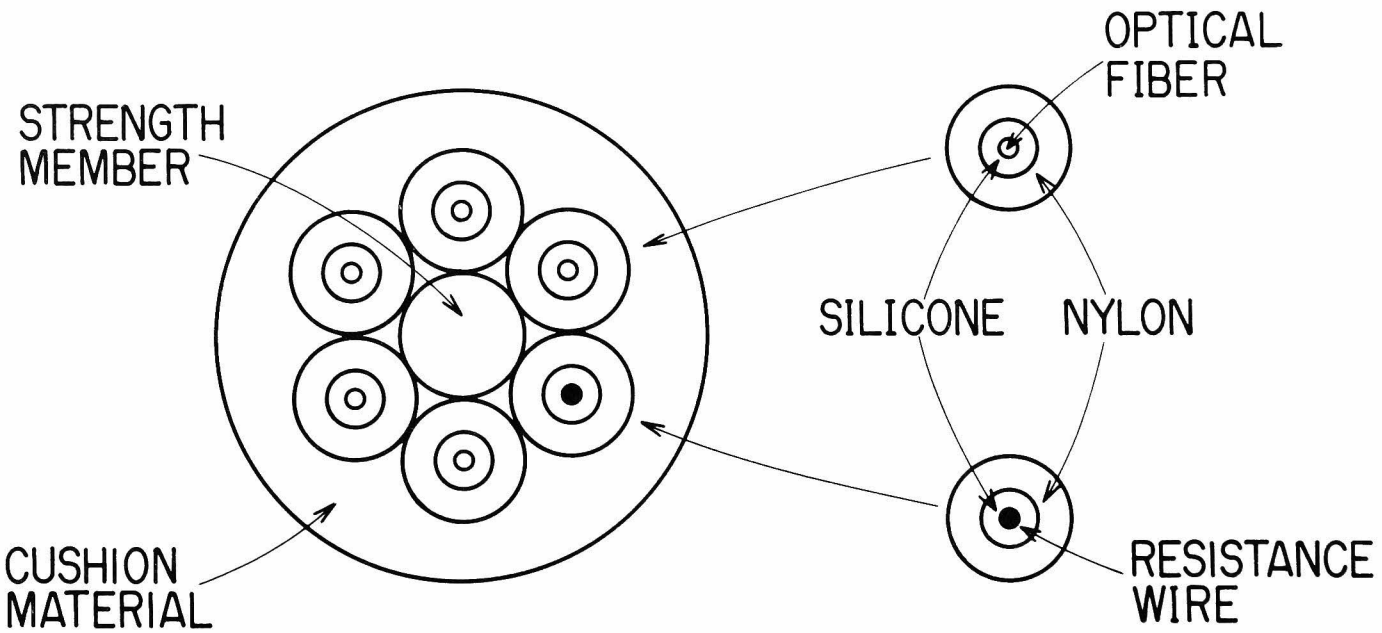

Fig. 5 Fiber unit containing both a coated wire and coated fibers.

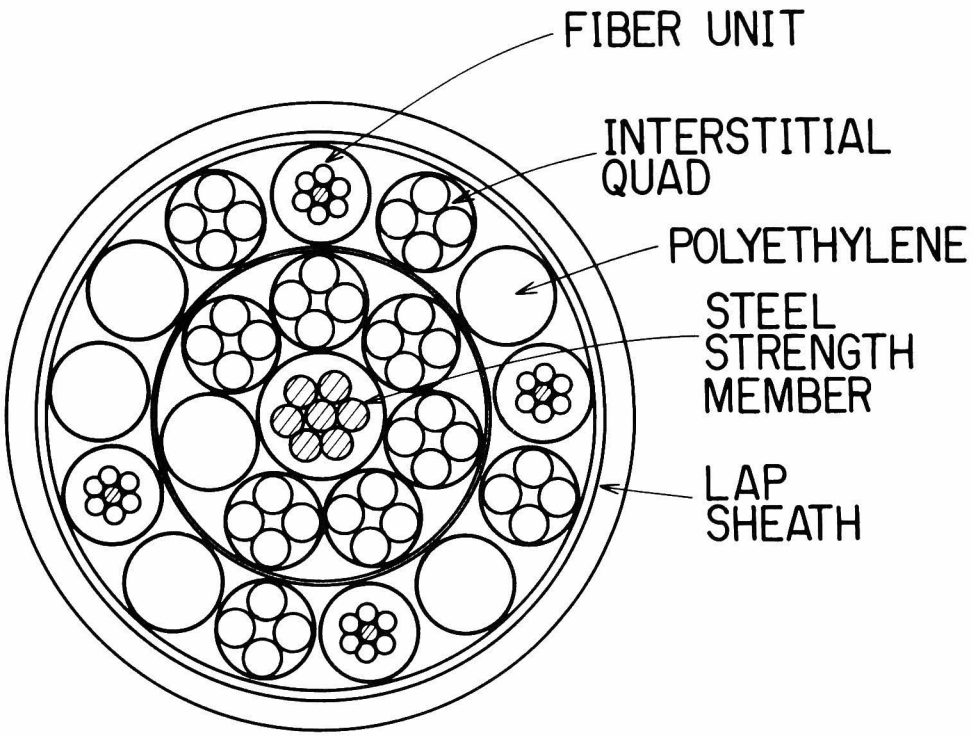

Fig. 6 Cross section of optical cable for strain measurement. This cable is a unit-type and laminated aluminum polyethylene sheath (LAP sheath) was used.

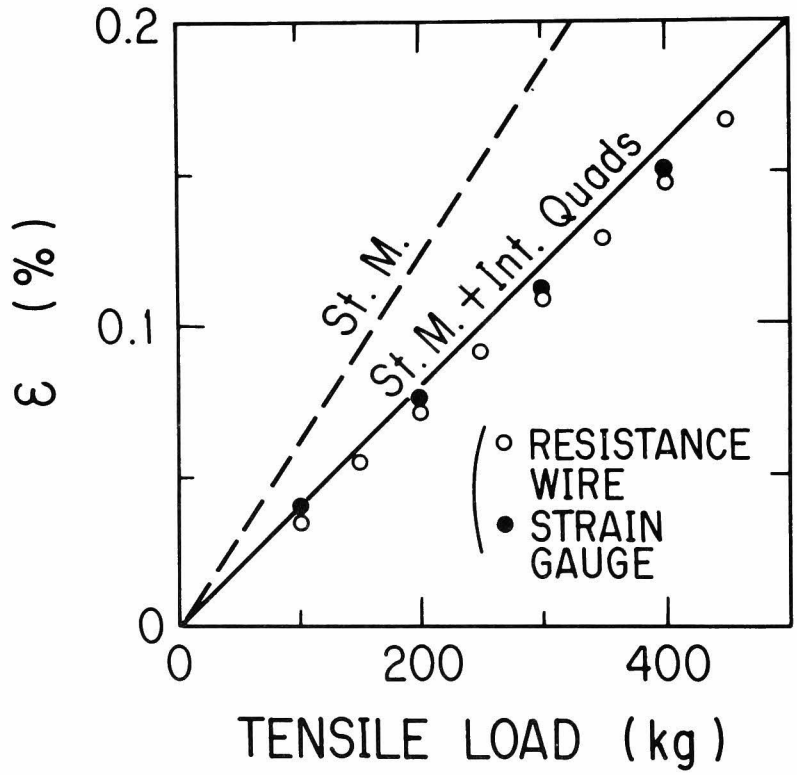

Fig. 7 Measured strain in the cable under tensile load.

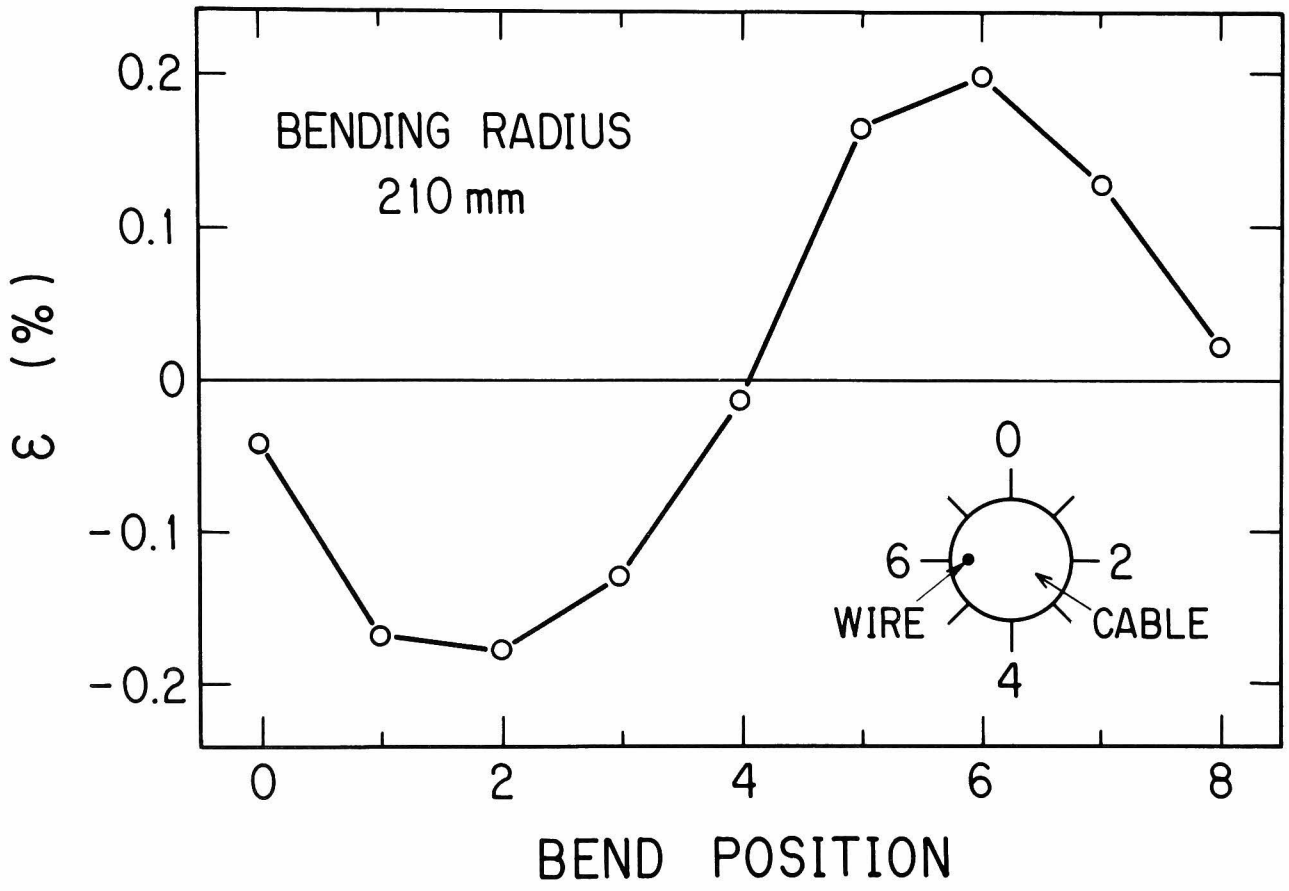

Fig. 8 Measured strain in the cable under bending.

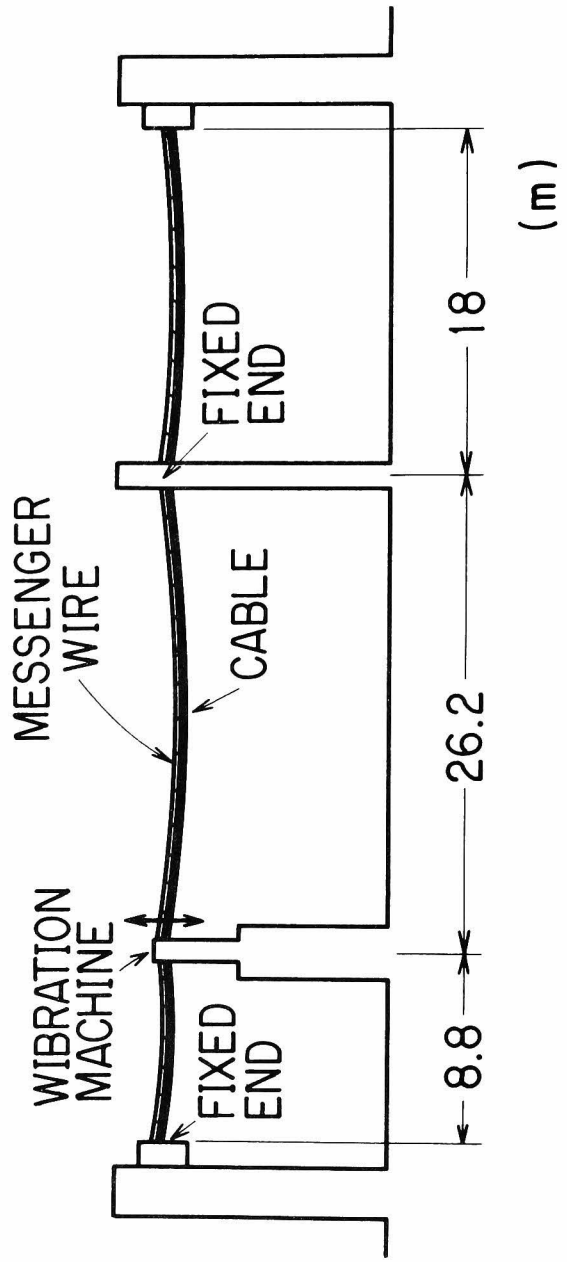

Fig. 9 Setup for vibration experiment.

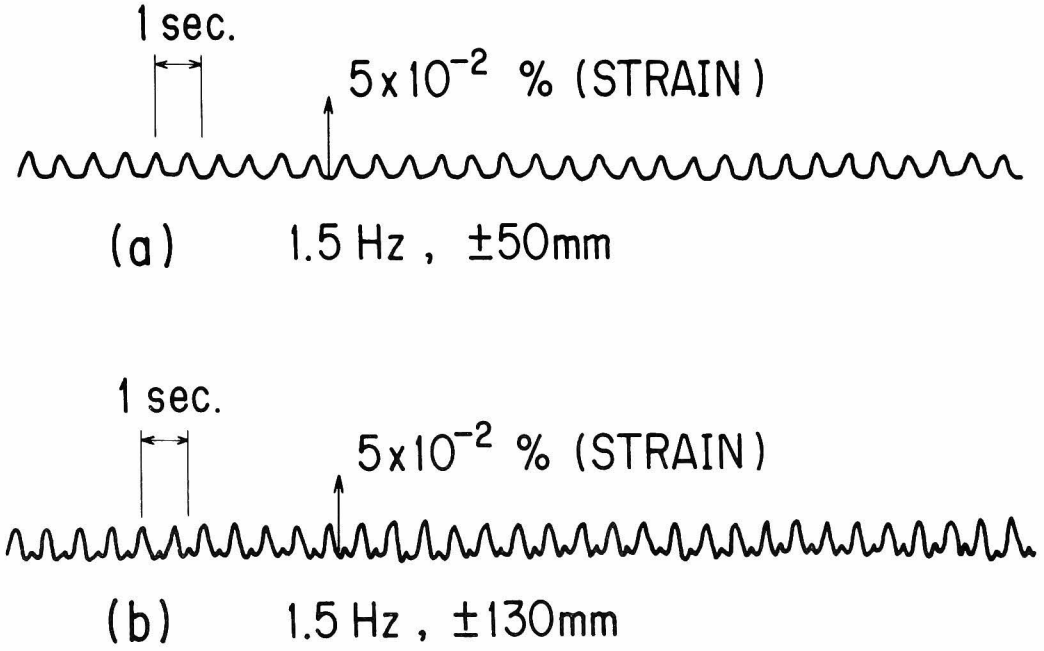

Fig. 10 Measured strain due to vibration.

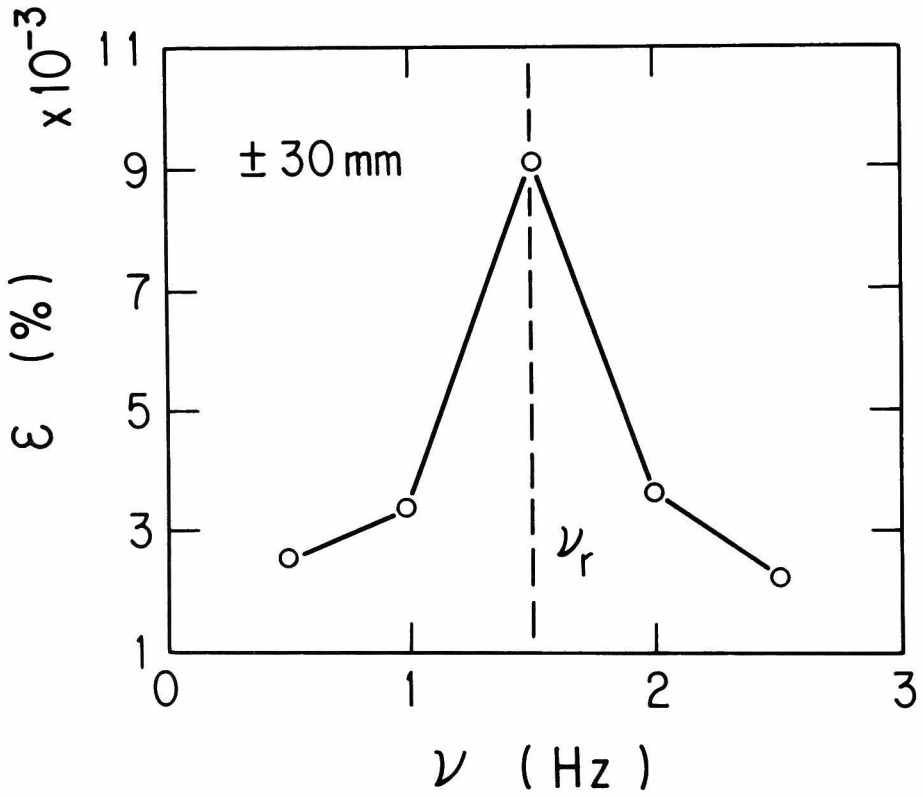

Fig. 11 Vibration frequency dependence of measured strain. The cable was vibrated with a amplitude of ± 30 mm.

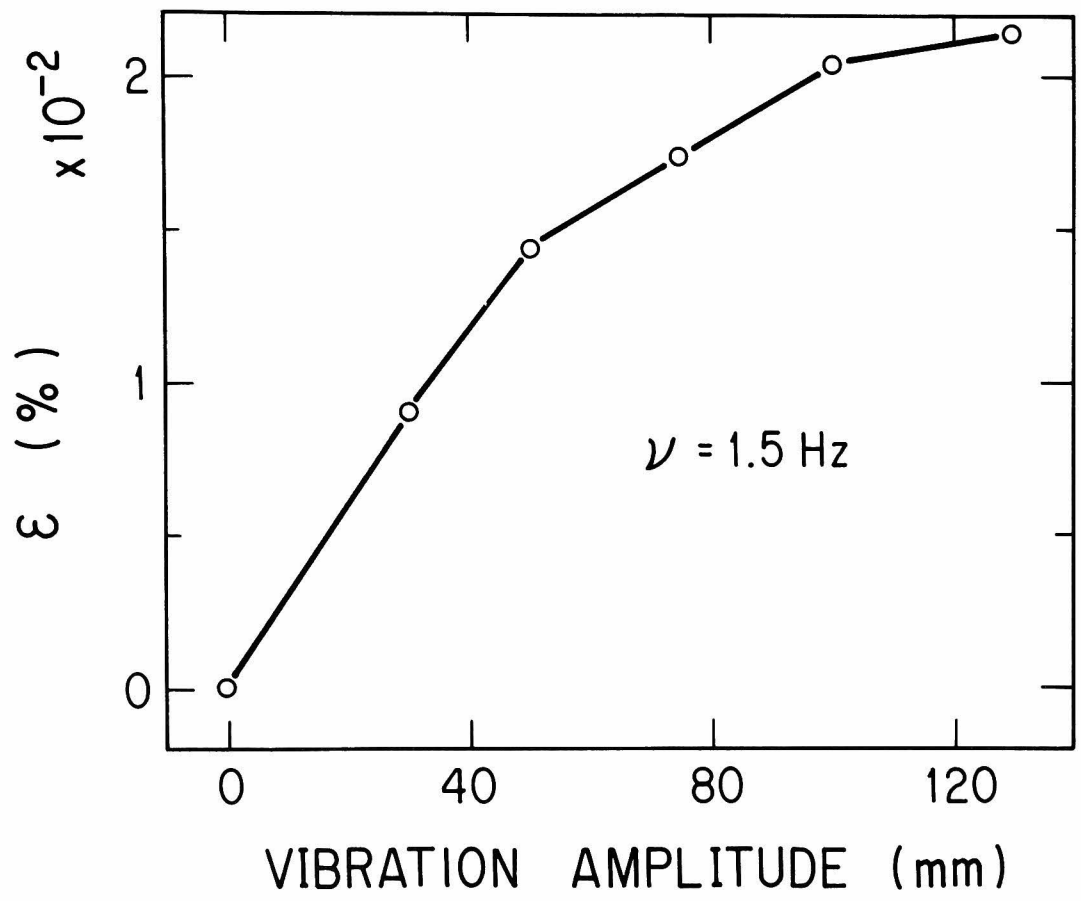

Fig. 12 Vibration amplitude dependence of measured strain.

CHAPTER IV TRANSMISSION LOSS OF COATED SINGLE-MODE FIBER AT LOW TEMPERATURES

Synopsis

Coated single-mode fibers with various coating thicknesses were manufactured, and loss increases due to cooling were measured. It was found that the excess loss increases steeply in the small V-value region at low temperatures. A simple model for fiber bends in the coating was introduced, and the increases in loss were related to the strain resulting from use of the model. It would appear that the axial compressive strain has a serious influence on the loss increases. A suitable silicone buffer layer for preventing loss increases has been determined. The selected silicone layer diameter is 0.45 mm for a 0.9-mm nylon outer layer diameter.

§1. Introduction

A single-mode optical fiber is an attractive transmission medium since it has broadband and low-loss [1] transmission characteristics. However, the transmission loss of a single-mode optical fiber cable tends to increase at low temperatures. Optical fibers are usually coated with plastic to preserve their strength, and compressive strain occurs in a fiber when the coated fiber is cooled. The compressive strain is caused by the large difference of thermal expansion coefficients between the optical fiber and the plastic coating. It has been reported that the fiber loss is seriously affected by an external force [2]. In reducing sensitivity to microbending losses, it has been predicted that a low-modulus buffer layer between the glass fiber and high-modulus coating is effective. A coated fiber structure with a silicone buffer layer was made [3] for multi-mode fibers, and fiber transmission losses seem to be stable at low temperatures. For single-mode fibers, optical loss characteristics at low temperatures are unclear. Moreover, it is necessary to clarify the relation between optical loss increase and cooling strain in the coated fiber. A suitable thickness of buffer layer is required to develop a stable optical cable.

In this chapter, loss increase characteristics of coated single-mode fibers are reported, and the buffer layer design is made on the basis of experimental and theoretical results. Coated single-mode fibers with different coating thicknesses were manufactured, and loss increases due to cooling were measured. Resistance wires coated with the same plastic material were also made. The cooling strain was evaluated by measuring the resistance changes in the coated wire. Then, the loss increases due to cooling strain were discussed together with the use of a fiber bending model to alloy this problem.

§2. Compressive Strain Measurements in Plastic-Coated Structures with a Resistance Wire

It is difficult to apply the conventional strain gauge to the measurement of fiber strain, because the optical fiber diameter is so very small. Thus, we made some coated resistance wire and measured the resistance changes instead of the strain gauge.

An axial strain in the wire causes a resistance change. The relation is given by [4]

$$\Delta R_e/R_e = K\varepsilon_z, \qquad (1)$$

where R_e, ΔR_e, ε_z, and K are wire resistance, resistance change, axial strain, and proportionality constant, respectively. The axial strain, therefore, is evaluated by Eq. (1) using the measured resistance change ΔR_e. The proportionality constant K is a known value of the wire material.

2.1 Resistance wire and measurement setup

A copper-nickel resistance wire was coated with the same plastic as the fiber coating material. The coated structures are shown in Fig. 1. Coated wires of different outer diameters were manufactured to investigate the influence of plastic contraction on the compressive strains due to cooling. The physical properties of the wire are listed in Table I.

The bridge circuit shown in Fig. 2 was used to measure resistance change. The coated wire length of 4.2 m was chosen so that the wire resistance R_e was equal to 120 Ω, which coincided with the value of the conventional strain gauge. A dummy wire without coating was used to cancel any error occurring due to the intrinsic thermal variation of wire resistance. A 4.2-m dummy wire length was also chosen, and both the coated and the dummy wires were laid in the same environmental conditions.

Thus, the strain due to coating contraction was correctly measured, and the error was attained within 10^{-6} in the -40 - +60 °C temperature region.

2.2 Strain measurements

First, the temperature dependence of the strain was measured for the plastic-coated wire of the two-layer structure. The result (circles) is shown in Fig. 3. After the bridge circuit was adjusted to a balance at 20 °C, the resistance change was measured for each temperature. The negative value represents compressive strain.

When the temperature changes by ΔT, the axial strain $\Delta\varepsilon$ in the wire due to the difference of thermal expansion coefficients between the wire and the plastic coating is given by

$$\Delta\varepsilon = \frac{E_2 A_2}{E_1 A_1 + E_2 A_2} (\alpha_2 - \alpha_1) \Delta T,$$

where E, A, and α are Young's modulus, cross-sectional area, and thermal expansion coefficient, and subscripts 1 and 2 indicate the central wire and coating, respectively. Since Young's modulus E_2 of the plastic coating changes

with temperature, the total strain at temperature T is given by

$$\varepsilon = (\alpha_2-\alpha_1)\int_{T_0}^{T} \frac{dT}{1+E_1A_1/E_2(T)A_2} , \qquad (2)$$

where T_0 is a standard temperature. The measured values of Young's modulus for nylon were 50, 200, and 210 kg/mm^2 at temperatures of 40, 0, and -40 °C, respectively. The calculated strain for the coated wire is also shown in Fig. 3, using the values listed in Table I. Calculated and measured results are in excellent agreement. It is concluded that the thermal strain in a coated fiber can be evaluated by Eq. (2) using the physical constants of fiber instead of those of the resistance wire.

Figure 4 shows the relation between the measured strain ε_m and the calculated value ε_c for two-layer and three-layer coated wire structures. The theoretical value ε_c for the three-layer structure was also estimated using Eq. (2) by neglecting the effect of the silicone layer, because Young's modulus was much smaller than that of nylon. Again calculated and measured values are found to agree, but a small discrepancy is observed for the three-layer structure. The measured strains

are smaller than the calculated values at low temperatures where the strain becomes compressive. The discrepancy may be caused by wire buckling in the coating. The compressive stress increases with lower temperature, and a buckling will occur when the compressive load becomes larger than the critical load [5]. Then the axial compressive strain will decrease due to wire bending. It is necessary to clarify the relation between fiber bending and cooling strain to evaluate the loss increases. Fiber bending at low temperatures will be discussed in Sec. 3.2 in connection with a bending model.

§3. Loss Increase in Coated Single-Mode Fibers Due to Cooling

3.1 Loss increase measurement

The optical loss was measured using an incoherent light source and a monochromator. A launching lens with N.A. = 0.4 was used. The optical power output from a fiber was detected with a Si P-I-N detector. The measurement fiber was wound into a coil about 300 mm in diameter. The five kinds of coated fiber listed in Table II were made. Type-1 coated fibers with different silicone-buffer layer outer diameters have the same 0.9-mm o.d. nylon coating. Type-2 coated fibers have the same

silicone diameter but different outer diameters of nylon coating. First, the optical losses at 20 °C were measured by varying the wavelength. Then, the coated fiber was cooled, and the optical losses were measured again. The loss increase due to cooling was evaluated by subtracting the loss at 20 °C. The optical loss of all the coated fibers at 20 °C was ∿3 dB/km at 0.85 μm. Figure 5 shows an example of the wavelength dependence of the loss increase as a function of temperature. It is clear from Fig. 5 that the optical loss increases steeply in the small normalized frequency (the so-called V-value) region. The loss increase pattern is similar to that due to cabling [6].

3.2 Fiber bending model

A three-layer coated wire was cooled to a temperature of -60 °C and was observed with a microscope. The diameters of silicone layer and nylon coating were 0.35 and 1.2 mm, respectively. Figure 6 shows the coated wire, and it is clear that the wire bends occurred within the plastic coating. Figure 7 shows a simple model of fiber bends at a low temperature. It is assumed that the fiber bends helically about the central axis due to the cooling contraction difference between the nylon

coating and the optical fiber. When a spiral bend occurs, the bending radius ρ is given by

$$\rho = \frac{R}{\cos^2\phi} , \qquad (3)$$

where R and ϕ are the spiral radius and the angle between fiber and a line perpendicular to the central axis, respectively (Fig. 7). When fiber buckling occurs, the strain difference between the fiber and the coating is given by

$$\varepsilon_d = \frac{L - p}{L} ,$$

where L and p are the fiber length and spiral pitch, respectively. Since the geometrical relation

$$\sin\phi = p/L$$

is valid, both equations lead to

$$\sin\phi = 1 - \varepsilon_d . \qquad (4)$$

The strain difference ε_d is a small quantity, and the following approximation holds:

$$\cos^2\phi = 1 - (1 - \varepsilon_d)^2$$
$$\simeq 2\varepsilon_d . \qquad (5)$$

Since the spiral radius R is related to the pitch p by

$$\frac{p}{2\pi R} = \tan\phi \ ,$$

R is given by

$$R \simeq \frac{p}{2\pi}\sqrt{2\varepsilon_d} \qquad (6)$$

using Eq. (5). Then the fiber bending radius ρ is expressed by

$$\rho \simeq \frac{p}{2\pi\sqrt{2\varepsilon_d}} \qquad (7)$$

using Eqs. (3), (5), and (6).

The contraction lengths of fiber and coating are the same unless fiber slip occurs during cooling. The strain caused in the fiber can be evaluated by Eq. (2). However, a strain difference occurs when fiber buckling takes place. The fiber subjected to a larger load than the critical value releases the excess strain, although the internal forces satisfy the equilibrium condition. The inference is in agreement with the measured strains shown in Fig. 4 for three-layer coatings. According to the buckling problem of a slender bar on an elastic foundation [5], the minimum critical load F_{min} causing fiber buckling and the spiral pitch p are given by [5]

$$F_{min} = r_f^2 \sqrt{\pi E_s E_f} , \qquad (8)$$

$$p = 2\pi r_f \sqrt[4]{\frac{\pi E_f}{4E_s}} , \qquad (9)$$

where r_f is the fiber radius, and E_s and E_f are Young's moduli of the silicone and of the fiber, respectively. The minimum strain ε_{min} and stress σ_{min} of the fiber corresponding to F_{min} is given by

$$\varepsilon_{min} = \frac{\sigma_{min}}{E_f} = \frac{F_{min}}{E_f \pi r_f^2} = \sqrt{\frac{E_s}{\pi E_f}} . \qquad (10)$$

Then the fiber bending radius ρ is given by

$$\rho = \frac{r_f}{\sqrt{2\varepsilon_d}} \sqrt[4]{\frac{\pi E_f}{4E_s}} \qquad (11)$$

using Eqs. (7) and (9). The value ε_d in Eq. (11) is estimated from the difference between cooling strain ε in Eq. (2) and minimum strain ε_{min} in Eq. (10):

$$\varepsilon_d = \varepsilon - \varepsilon_{min} . \qquad (12)$$

As a result, ρ is calculated by Eqs. (11) and (12).

Figure 8 shows the calculated cooling strain ε, the minimum strain ε_{min}, and the bending radius ρ for the coated

fiber 1-3. A standard temperature of 20 °C was chosen. The minimum strain ε_{min} depends on temperature, since Young's modulus of silicone E_s varies with temperature. The E_s values used were measured as 0.31, 0.18, 0.10 kg/mm^2 at temperatures of -60, -40, and 0 °C, respectively. It is clearly seen in Fig. 8 that the bending radius decreases with lower temperature.

3.3 Relation between loss increase and bending radius at low temperature

Figure 9 shows the measured temperature dependence of the V-value giving 1-dB/km loss increase for three coated fibers. Theoretical values are also shown by solid curves in Fig. 9 given by the above mentioned bending model and a curvature loss formula [7]. The loss α_{01} for the LP_{01} mode is given by

$$\alpha_{01} = \frac{\sqrt{\pi}\,\kappa^2 \exp[-2/3\ (\gamma^3/\beta^2)\rho]}{2\gamma^{3/2}\ V^2\sqrt{\rho}\ K_{-1}(\gamma a)K_1(\gamma a)}\ , \qquad (13)$$

where β is the axial propagation constant, and κ and γ are the transverse propagation constants in the core and the cladding, respectively. $K_{\pm 1}(z)$ is the modified Bessel function, and V and a are the V-value and the core radius of the fiber, respectively. It is found from Fig. 9 that

the experimental results are in good agreement with the theoretical curves. It is concluded that the fiber bending model and the curvature loss formula can represent loss increase characteristics of a coated single-mode fiber due to cooling. A fiber in a coating is subjected to both axial and radial compressive stresses when it is kept at low temperature. However, it is believed that the radial compressive stress does not cause the displacement of the fiber axis. An axial compressive stress, on the contrary, causes fiber bend and consequently loss increase. This speculation is consistent with the fact that the present bending model well represents the measured loss increase by considering only axial strain.

§4. Suitable Silicone Diameter in a Three-Layer Structure

For the design of coated fiber structure, it is necessary to determine nylon coating and silicone layer diameters from the viewpoint of preventing a loss increase at low temperatures. First, a nylon coating diameter of 0.9 mm was selected. The value was adopted in a short-haul fiber transmission system field trial [8] using multi-mode fibers. Here a suitable silicone layer diameter will be selected causing a negligibly small loss increase at low temperatures.

Figure 10 shows the calculated bending radius as a function of the silicone layer diameter. Calculations were made using Eqs. (2), and (10) - (12) for a constant nylon coating diameter of 0.9 mm. The results show that the bending radius becomes small with decreasing silicone layer diameter because of large forces due to nylon contraction.

Experimental loss increases as a function of the silicone layer diameter are shown in Fig. 11 at a temperature of -40 °C, which is considered the lowest temperature for cables installed in a natural environment. Measurements were made for three kinds of coated fiber, that is, 1-1, 1-2, and 1-3 as listed in Table II. A loss increase calculation was made using the fiber bending radius in Fig. 10 and the loss formula (13). The calculated values are shown by solid curves and are in good agreement with the experimental values.

A suitable silicone layer diameter giving a small loss increase, for example, 0.2 dB/km at a temperature of -40 °C, is now discussed. The loss increase strongly depends on the fiber parameters, the relative index difference Δ, and the V-value. Suitable parameters, which minimize cabling and splicing loss increases, have been proposed [6], and the values have been determined as

Δ = 0.2 % and V = 2.2. The core diameter 2a is 6.5 μm at a wavelength of 0.85 μm and 9.9 μm at 1.3 μm, assuming that the index profile is a perfect step-index type. Using the values Δ = 0.2 % and 2a = 6.5 μm, loss increase was calculated in terms of silicone layer diameter and V-value. The result is shown in Fig. 12. Here the solid curve indicates the loss increase of 0.2 dB/km, and smaller loss increases occur in the hatched region. It is clear from Fig. 12 that the suitable silicone layer diameter for V = 2.2 is 0.41 mm. Since the excess loss increases steeply for small values of V as shown in Fig. 11, a 0.45-mm silicone layer diameter is preferable, giving a little safety margin in the V-value.

§5. Conclusion

Coated single-mode fibers with different coating diameters were manufactured, and loss increases due to cooling were measured. It was found that the loss increases steeply in the small V-value region at low temperatures.

Compressive strain in a coated fiber has been evaluated using resistance wire. A simple model for explaining fiber bending was introduced, based on measured compressive strain. The loss increase was related by

using the model to the compressive strain due to cooling. It was found that experimental loss increases agree well with the calculated values, and we have shown that the axial compressive strain has a serious influence on the loss increase of coated fibers during cooling. Therefore, a silicone diameter should be determined to decrease the cooling stress. A suitable silicone layer diameter, which causes negligibly small loss increases, was found to be 0.45 mm for a fiber with 0.125-mm o.d., 0.2 % relative index difference, 2.2 V-value, coated with nylon of 0.9-mm diam.

References

1. A. Kawana, T. Miyashita, M. Nakahara, M. Kawachi, and T. Hosaka: 'Fabrication of low-loss single-mode fibres', Electron. Lett., 13, 7, p.188 (1977)
2. D. Gloge: 'Optical-fiber packaging and its influence on fiber straightness and loss', Bell Syst. Tech. J., 54, 2, p.245 (1975)
3. T. Naruse, Y. Sugawara, and K. Masuno: 'Nylon-jacketed optical fibre with silicone buffer layer', Electron. Lett., 13, 6, p.153 (1977)
4. See, for example, I. Vigness: 'Investigation of stress-strain relations of metal wires by electrical resistance changes', J. Appl. Phys., 23, 1, p.43 (1952)
5. See, for example, S. P. Timoshenko, 'Theory of Elastic Stability', (McGraw-Hill, New York, 1961)
6. Y. Katsuyama, S. Mochizuki, K. Ishihara, and T. Miyashita: 'Single-mode optical fiber cable', Appl. Opt., 18, 13, p.2232 (1979)
7. D. Marcuse: 'Curvature loss formula for optical fibers', J. Opt. Soc. Am., 66, 31, p.216 (1976)
8. K. Ishihara, M. Tokuda, and S. Seikai: '48 core optical fiber cable design and characteristics', Rev. Electr. Commun. Lab. NTT Jpn., 27, 11-12, p.949 (1979)

Table I. Physical Properties of Experimental Material.

	Resistance wire	Optical fiber	Nylon
Thermal expansion coefficient (/°C)	1.6×10^{-5}	5.5×10^{-7}	1×10^{-4}
Young's modulus (kg/mm^2)	1.6×10^{4}	7.3×10^{3}	*
Specific resistance ($\Omega \cdot cm$)	5.05×10^{-5}	——	——

* It varies with temperature. (See text)

Table II. Coated Single-Mode Fiber Used in the Experiment.

	Coated fiber	Core diameter (μm)	Relative index difference (%)	Fiber diameter (μm)	Silicone diameter (mm)	Nylon diameter (mm)	Fiber length (m)
Type 1	1-1	5.8	0.2	125	0.34	0.9	195
	1-2				0.39		
	1-3				0.50		
Type 2	2-1	5.8	0.22	150	0.45	1.2	203
	2-2					1.1	

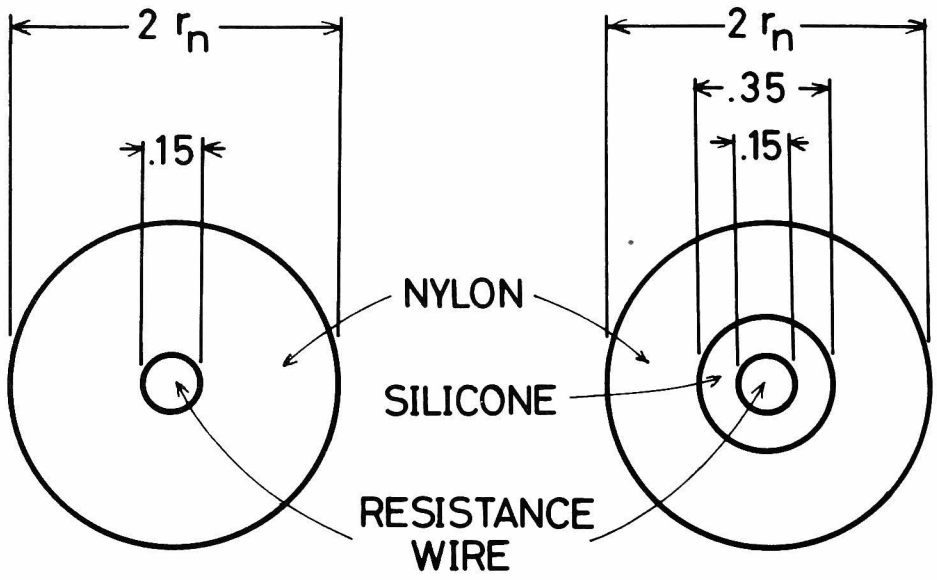

Fig. 1 Coated resistance wire structures.

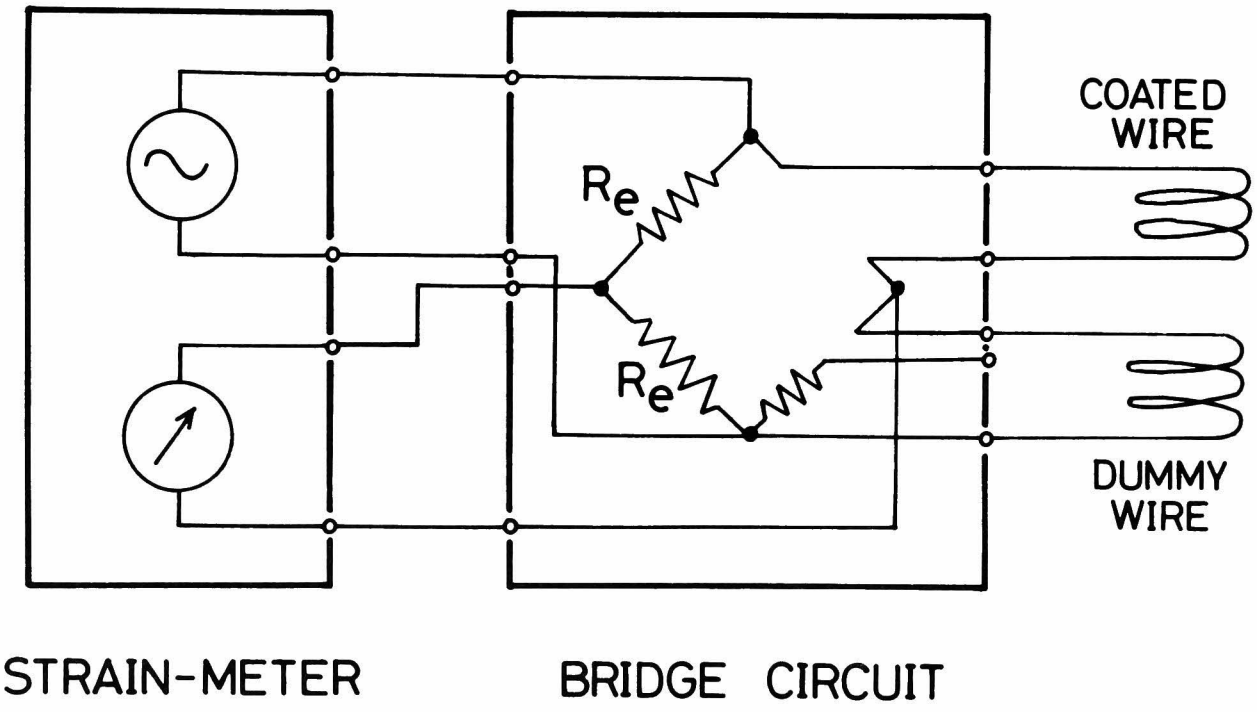

Fig. 2 Setup for measuring resistance change. Thermal strains were measured for a coated resistance wire. A dummy resistance wire without coating was used to cancel the error due to the intrinsic thermal resistance coefficient of the wire.

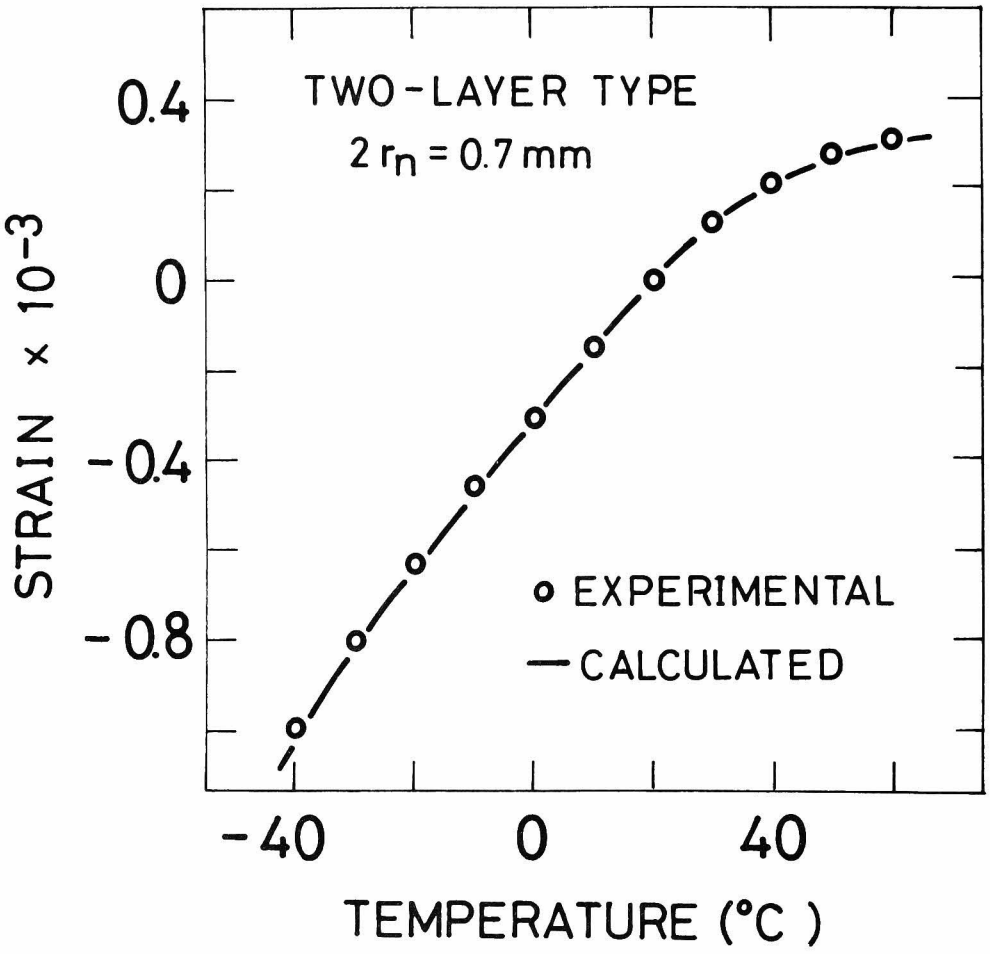

Fig. 3 Temperature dependence of thermal strain measured with the resistance wire.

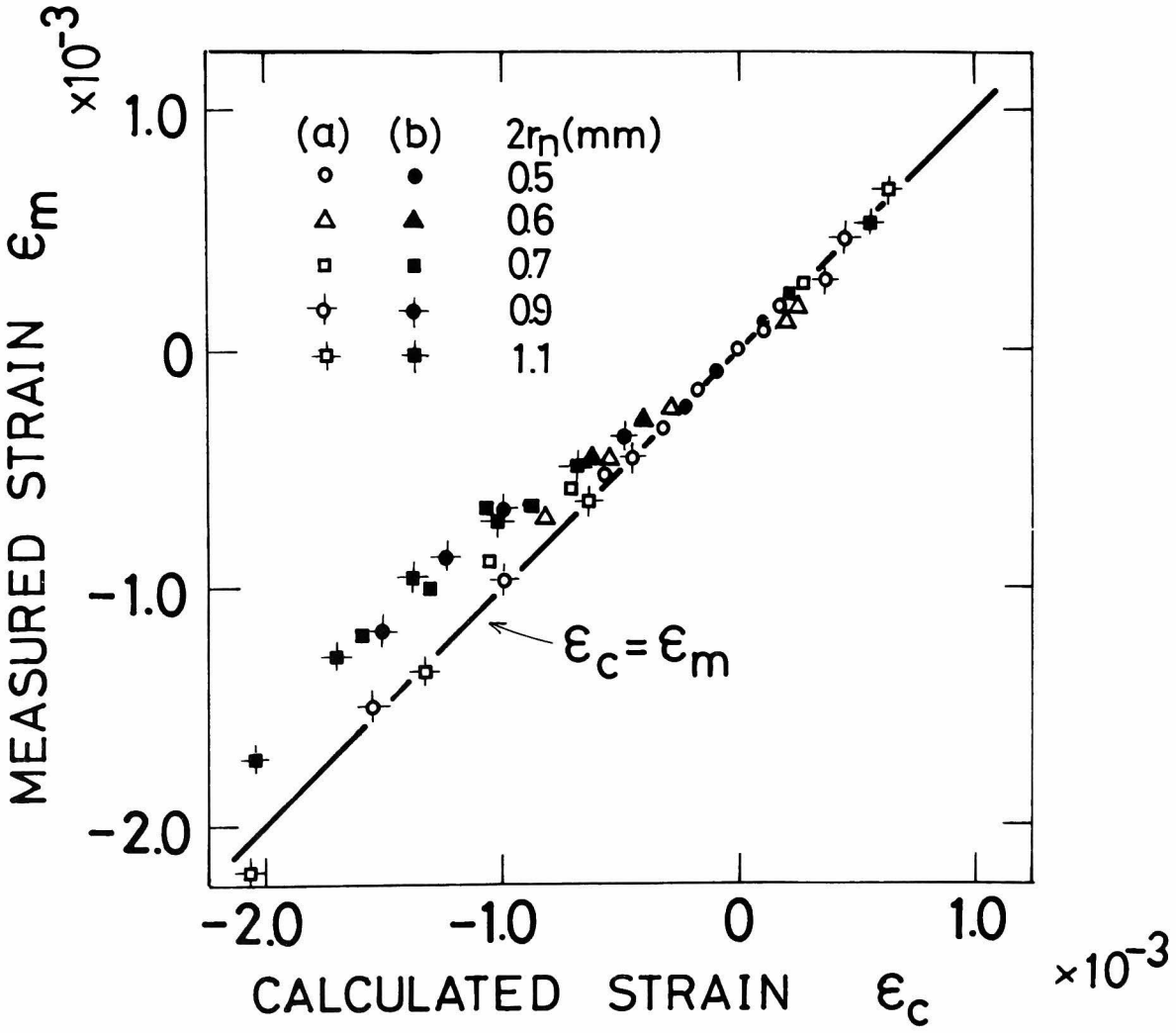

Fig. 4 Comparison between measured and calculated strains for (a) two-layer and (b) three-layer structures.

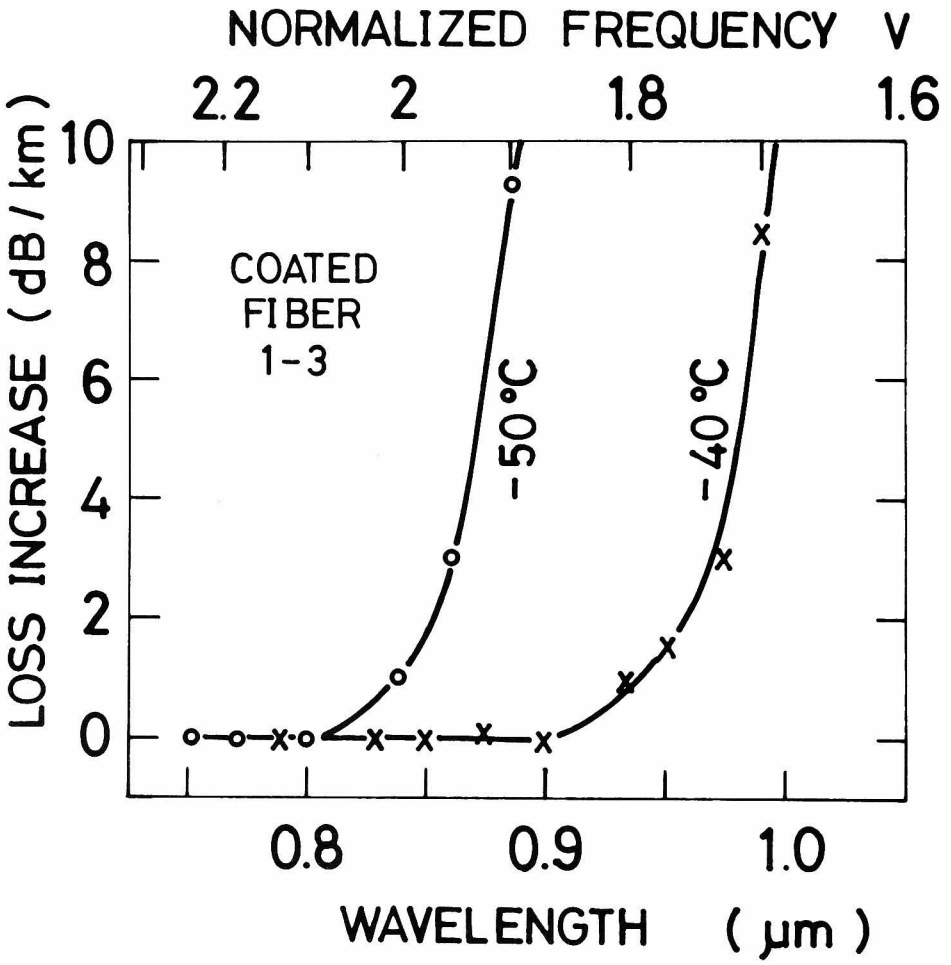

Fig. 5 Loss increase characteristics of a coated single-mode fiber due to cooling.

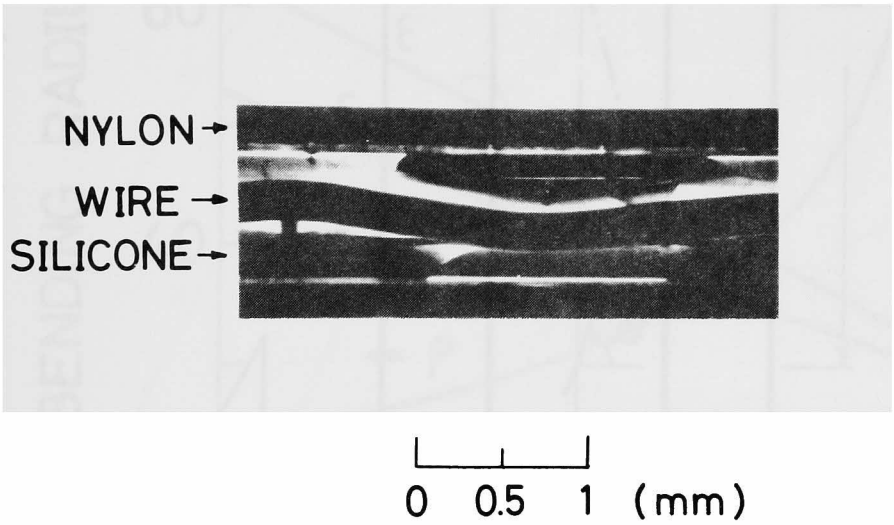

Fig. 6 Resistance wire bend in the coating at a temperature of -60 °C.

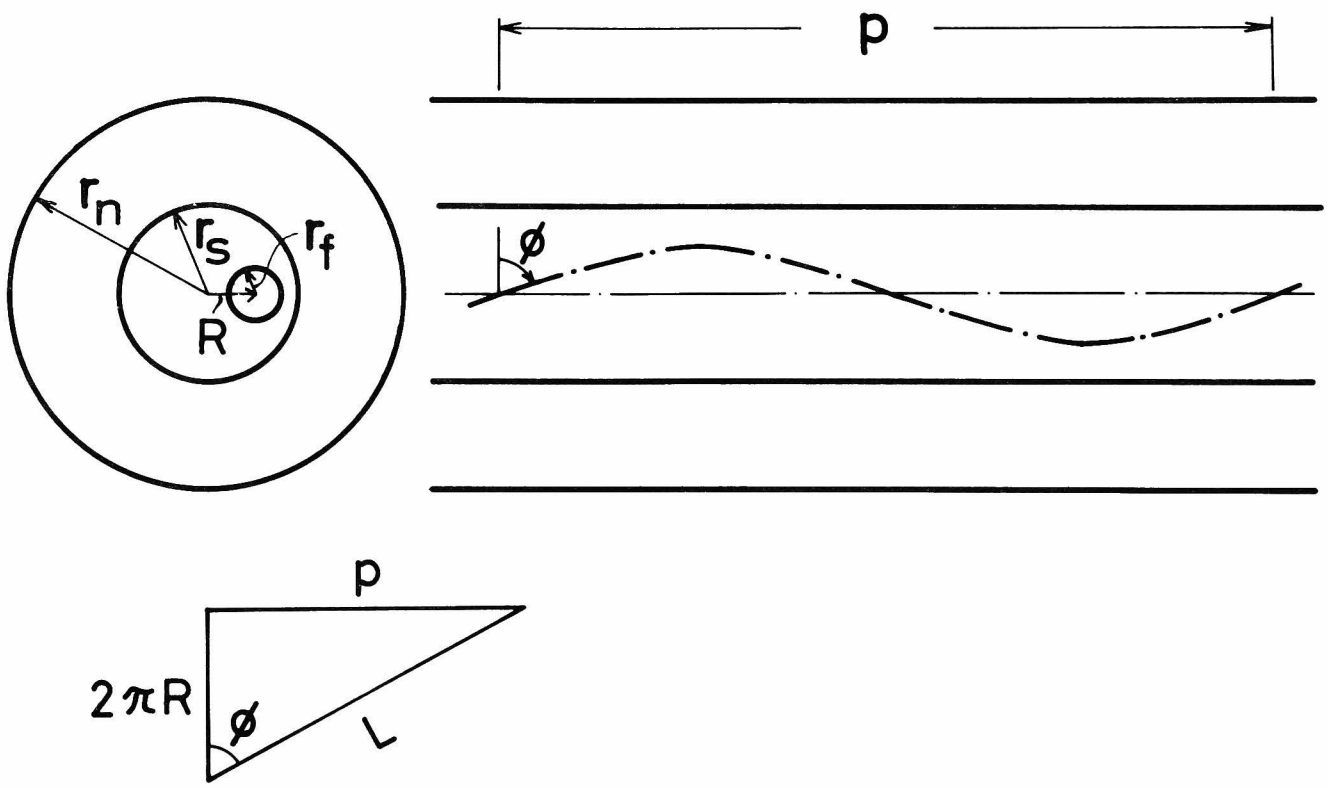

Fig. 7 Fiber bending model to evaluate loss increase.

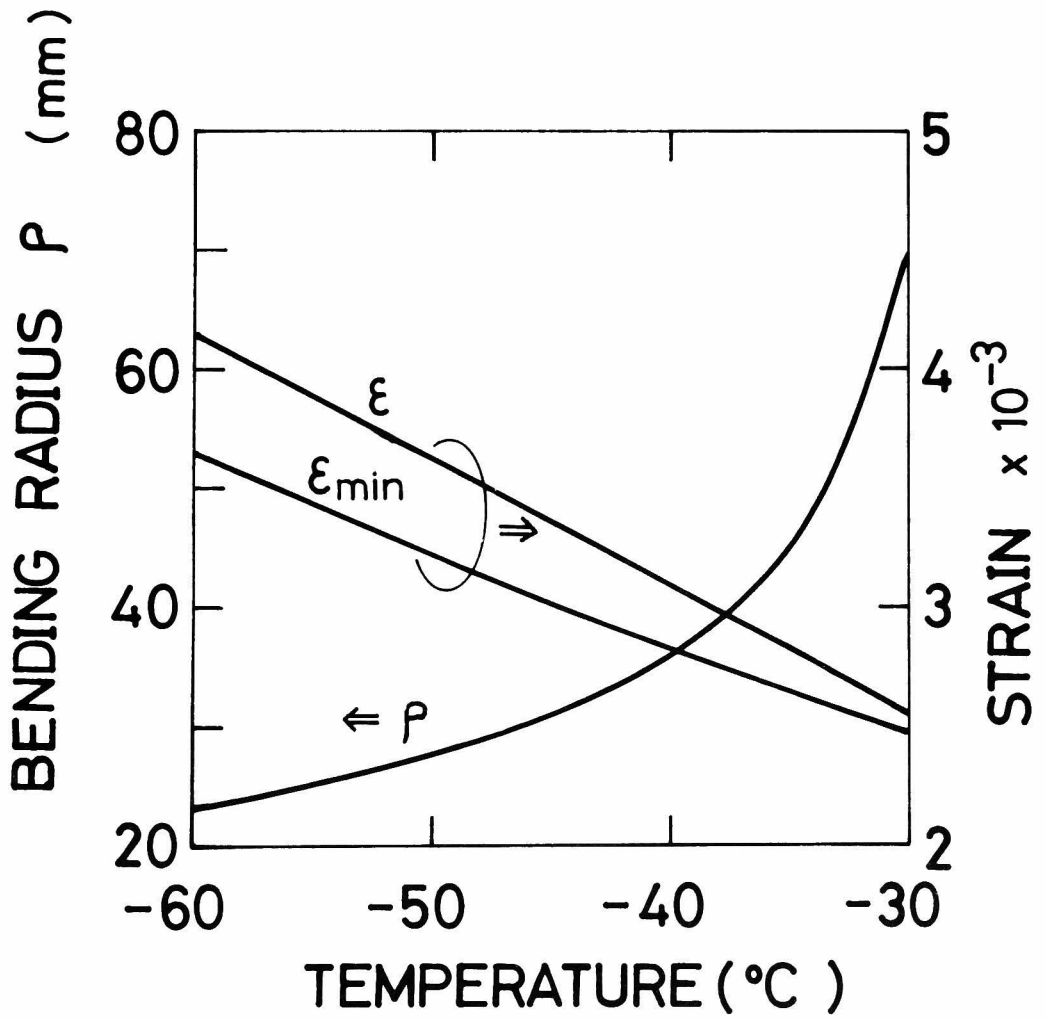

Fig. 8 Calculated fiber strain ε and bending radius ρ for a coated fiber with 0.9-mm nylon, 0.5-mm silicone, and 0.125-mm fiber diameters.

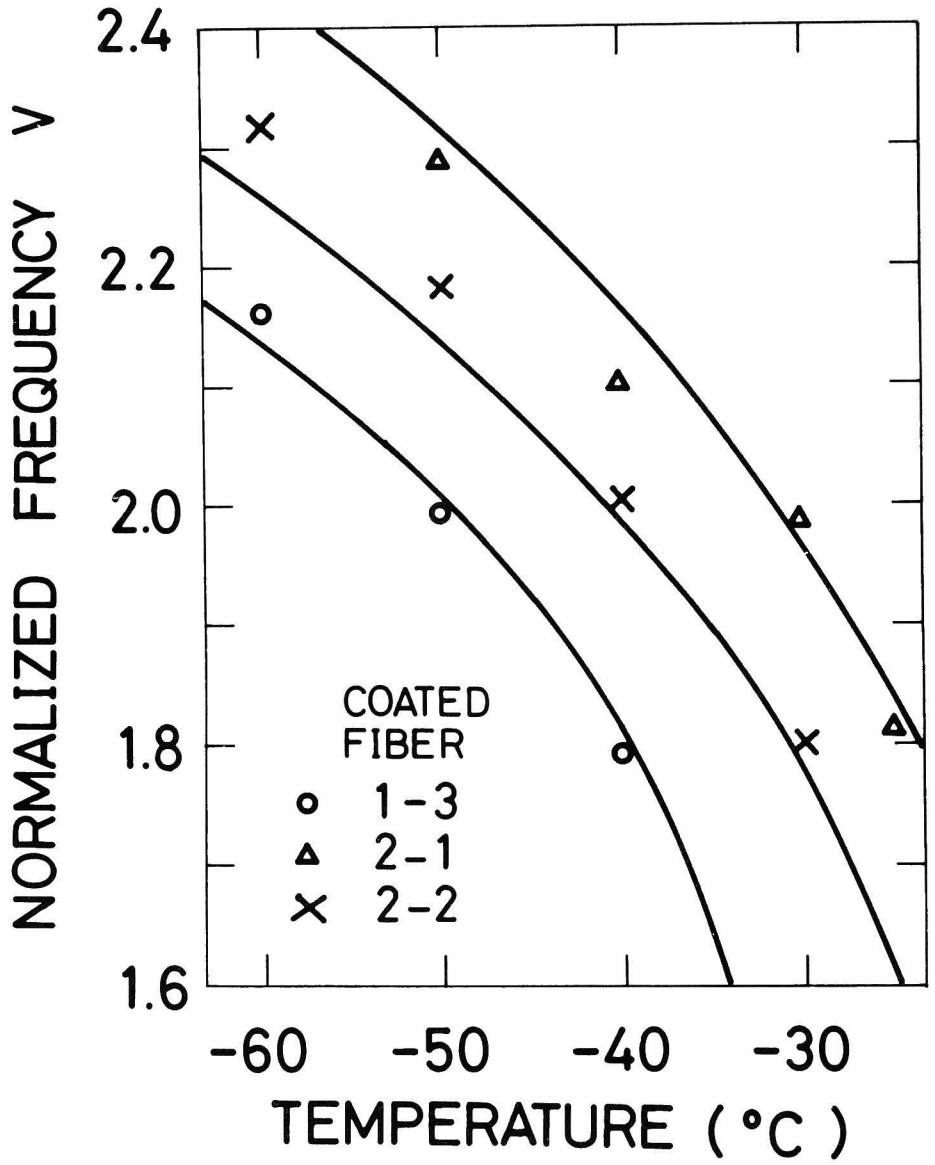

Fig. 9 Comparison of calculated and measured V-values giving 1-dB/km loss increase.

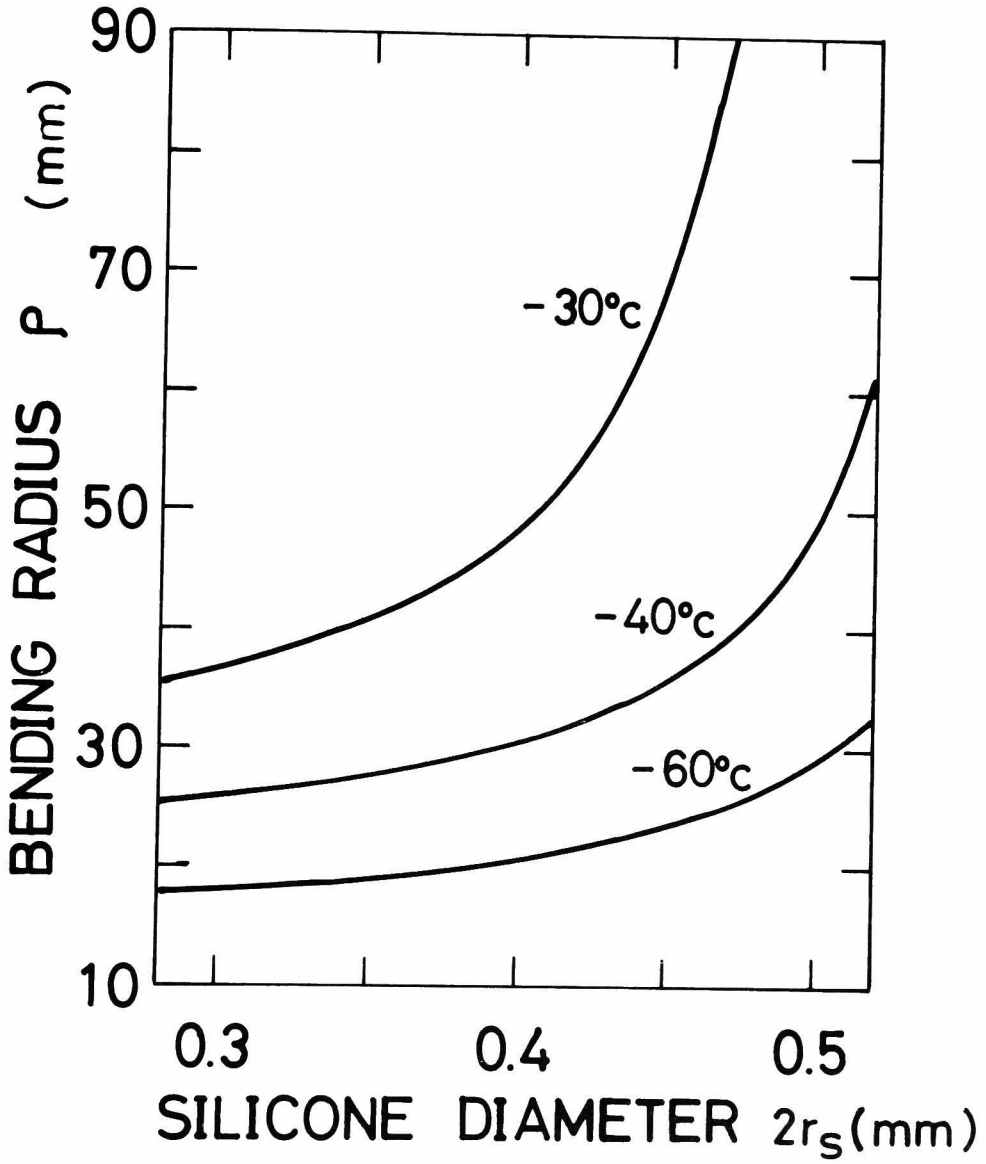

Fig. 10 Calculated bending radius as a function of the silicone layer diameter for coated fibers with 0.9-mm nylon coating diam. and 0.125-mm fiber diam.

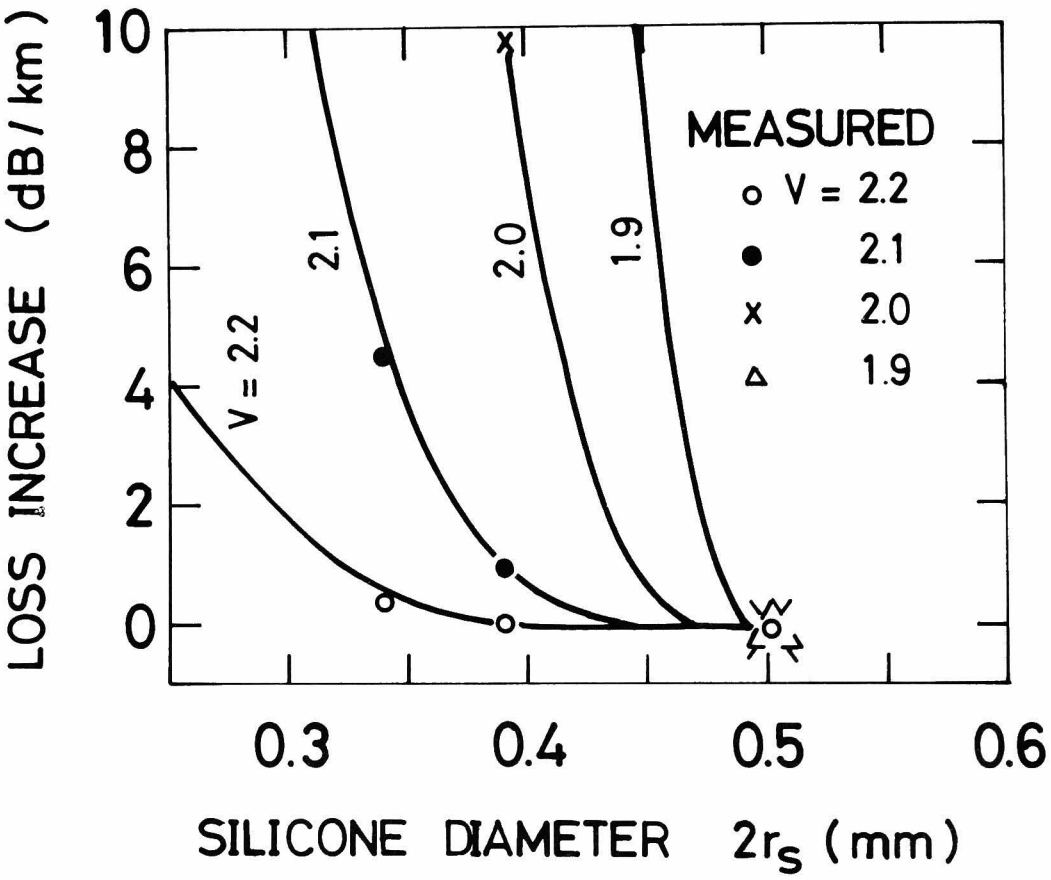

Fig. 11 Calculated and measured loss increases as a function of silicone layer diameter. The V-value is taken as a parameter.

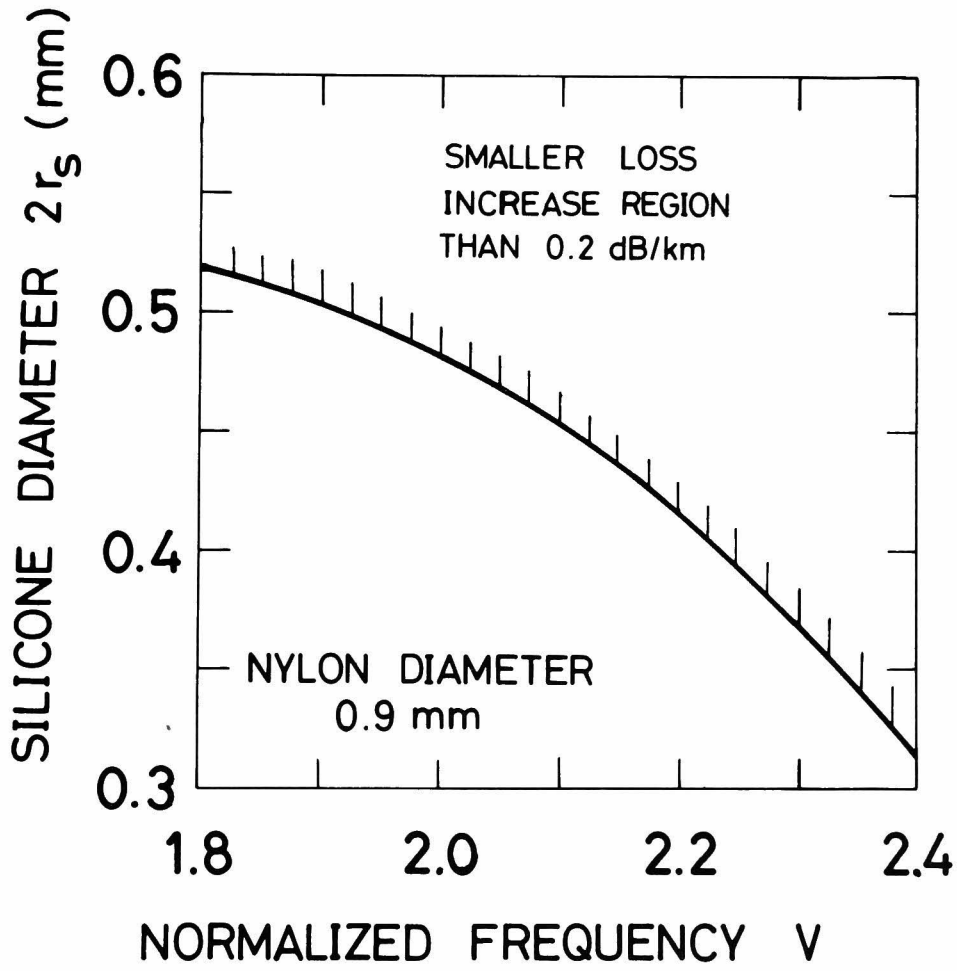

Fig. 12 Calculated suitable silicone layer diameter that causes small loss increases.

CHAPTER V CONCLUSION

Design and performance studies on single-mode optical fiber cable were described. The purpose of the cable design is that the cable possesses (1) enough mechanical strength and (2) stable transmission characteristics without loss increase. Several single-mode optical fiber cables were manufactured, and loss increase and mechanical properties were examined. The cable structure without loss increase during manufacturing process has been attained by a suitable selection of fiber parameters. The loss stability at low temperatures was examined for coated fibers with silicone buffer layer. The loss increase was found to be related to the cooling strain due to nylon contraction. The suitable value of silicone layer outer diameter has been determined from the viewpoint of preventing a loss increase. The fiber strain inside the cable under several loads, tension, bending, and vibration has been evaluated by a novel resistance wire method. Measured results have verified that the cable has enough mechanical strength to be used in the natural environment.

As a result of the present studies, suitable cable structure for single-mode fiber has been determined. The main points of the cable structure are as follows; (1) fiber parameters: Δ=0.2 % and V=2.2, (2) nylon coated fiber structure with silicone buffer layer, (3) central

strength member, and (4) strand-structure with the coated fibers.

Acknowledgments

The author would like to express his sincere gratitude to Professor K. Fukuda, Kyoto University, for his guidance and encouragements throughout this work. The author also thanks Professor M. Oyane and Professor J. Ikenoue, Kyoto University, for their suggestions and guidance.

The author wishes to express his thank to Professor G. Marubayashi, Nagaoka science and technology College, Mr. H. Fukutomi, Mr. K. Masuno and N. Kojima for their supports and encouragements throughout this study. The author is much indebted to Dr. Y. Kato and Dr. N. Uchida for many helpful comments and discussions. Especially, Dr. N. Uchida reviewed the manuscripts carefully and pointed out many fruitful suggestions. Mr. Y. Ishida and Mr. K. Ishihara are the leader of the fiber cable project in ECL where this work has been made and the author wishes to sincere thank to them for their continuous guidance. He also thanks his co-workers in his laboratory, especially to Mr. Y. Mitsunaga and Mr. S. Mochizuki for their experimental cooperation. Thanks are also due to Mr. M. Tokuda for the supports for optical loss measurements.

APPENDIX A NEW METHOD FOR MEASURING V-VALUE OF A SINGLE-MODE OPTICAL FIBER

Synopsis

A simple method is proposed for the direct measurement of the V-value for a single-mode optical fiber. This method consists of measurement of loss peaks, corresponding to cutoff wavelengths of the higher modes, which are easily observed for a fiber with a bend.

It is important to measure the normalized frequency (the so-called V-value) of a single-mode optical fiber, because the number and propagation characteristics of guided modes in the fiber are determined by the V-value:

$$V \simeq 2\pi a\sqrt{2n\Delta n}/\lambda, \qquad (1)$$

where n is the refractive index of the fiber, Δn is the index difference between the core and cladding, a is the core radius, and λ is the optical wavelength. Determination of the V-value is usually made by measuring Δn and a. However, the accuracy of measurements is insufficient at present for the precise determination of the V-value, because the structure of a single-mode fiber is very fine. In this section, we propose a new method for the direct measurement of the V-value and discuss the applicability of the method.

When a single-mode optical fiber is bent, loss peaks appear, corresponding to the cutoff of higher modes. The radiation loss due to curvature in a single-mode fiber with sinusoidal bends, for example, is given by Ankiewicz [1]. Figure 1 shows the wavelength dependence of the loss caused by the curvature calculated by using his theory [1] for an appropriate combination of fiber parameters and bend parameters. Here the LP mode [2] is used for simplicity, and the mode power distribution in the multi-

mode region is assumed to be uniform. As a higher mode approaches its cutoff, the loss increases steeply. At the cutoff wavelength, the loss reaches a maximum and then suddenly reduces to zero. Thus the longest wavelength in each peak corresponds to the cutoff wavelength. Such behavior will generally occur due to any kinds of bend or pressure.

The normalized cutoff frequency V_c corresponding to each mode is calculated by using the characteristic equation of the mode. Therefore, it is possible to determine the V-value at a given wavelength λ by

$$V = V_c \lambda_c / \lambda \qquad (2)$$

using a measured value of the cutoff wavelength λ_c.

A measurement of λ_c was made by the folloing procedure. A single-mode optical fiber of a few meters in length was kept almost straight and the output optical power from the fiber was measured by varying the wavelength. The fiber was bent circularly by one full turn and the output power was measured again. The condition of excitation to the fiber was unaltered during this procedure. The radius of the circular bend was usually chosen to be 10 to 100 mm. Comparing the wavelength dependence of the output optical power for the bent fiber with that for the straight

fiber, the additional loss due to the bend at the cutoff was evaluated. We used a monochromator for the selection of optical wavelength, and the resolvability of the wavelength was approximately 50 Å.

The measurement was made for the three kinds of fiber listed in Table I. The fiber parameters Δn and a were estimated from the values of the preform rods and were measured by a conventional method using an interference microscope. The loss peaks for fiber A measured by the present method are shown in Fig. 2. Mode identification of the peaks was made by considering the separation between the peaks, as well as the V-value estimated from Δn and a. It is found that the measured loss does not rise perpendicularly at λ_c, contrary to the theoretical expectation. The reason may be because the excitation efficiency of a higher mode becomes low as the mode approaches its cutoff and also the propagation loss of the higher mode is large near cutoff, even for the straight fiber. Thus we chose the rising point (the longest wavelength) to be λ_c. Peak values of the loss are small for the higher modes, and this fact is qualitatively explained by considering the number of modes contained in each LP mode.

Measured λ_c and $V_c\lambda_c$ are summarized in Table II for fiber A. Here we consider V_c for an ideal circular fiber

with a step-index profile. We may expect $V_c\lambda_c$ to be constant for all higher modes within the measured wavelength region, because the dispersions of n and Δn are negligibly small. The measured values of $V_c\lambda_c$ are in good agreement with each other, within a few percent, except for the value in parentheses, which is not accurate, owing to the tail of the loss peak for the LP_{31} mode. Similar measurements were made for fibers B and C, and the results are shown in the last column of Table I. For fiber B, only one peak was observed in the wavelength region between 0.5 and 1.1 μm, which we presume to be the peak for the LP_{11} mode by considering the estimated fiber parameters.

In conclusion, we have proposed a new method for the precise determination of the V-value in single-mode optical fibers by utilizing the loss increase at the cutoff of a higher mode due to a bend. The main advantage of the method is that the effective V-value is essentially measured for a fiber with any type of a refractive index profile. The method is simple in principle and in procedure, and high accuracy is expected for the measured V-value. At present, the accuracy is estimated to be within a few percent and is mainly limited by uncertainty of the rising point in loss peak. It is also advantageous that the fiber length required for the measurement is only a few meters.

References

1. A. Ankiewicz: 'Radiation losses from sinusoidal serpentine bends in optical waveguides', Electron. Lett., 11, 1, p.30 (1975)

2. D. Gloge: 'Weakly guiding fibers', Appl. Opt., 10, 10, p.2252 (1971)

Table I. Fiber paramaters and measured values of $V_c\lambda_c$.

Fiber	Core diameter 2a (μm)	Index difference Δn/n (%)	Estimated $V_c\lambda_c$ (μm)	Measured $V_c\lambda_c$ (μm)
A	8.0	0.3	2.8	3.11
B	5.0	0.25	1.6	1.52
C	4.6	0.45	2.0	2.04

Table II. Measured values of λ_c and $V_c\lambda_c$ for fiber A.

Mode	V_c	Measured				Estimated
		R = 11 mm		R = 15 mm		
		λ_c(μm)	$V_c\lambda_c$(μm)	λ_c(μm)	$V_c\lambda_c$(μm)	λ_c(μm)
LP_{11}	2.405	—	—	—	—	1.18
LP_{02}, LP_{21}	3.832	0.82	3.14	0.81	3.10	0.74
LP_{31}	5.136	0.61	3.13	0.61	3.13	0.55
LP_{12}	5.520	(0.53)	(2.93)	0.55	3.04	0.51

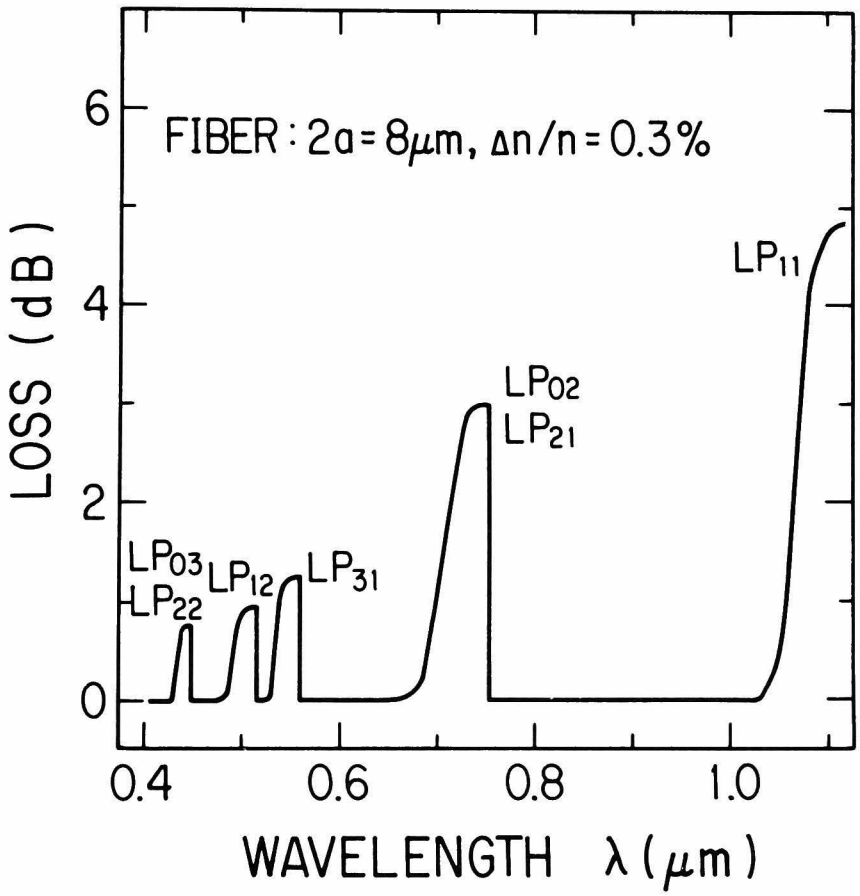

Fig. 1 Calculated wavelength dependence of loss caused by sinusoidal bends. Amplitude of bend = 0.425 mm, pitch = 50 mm.

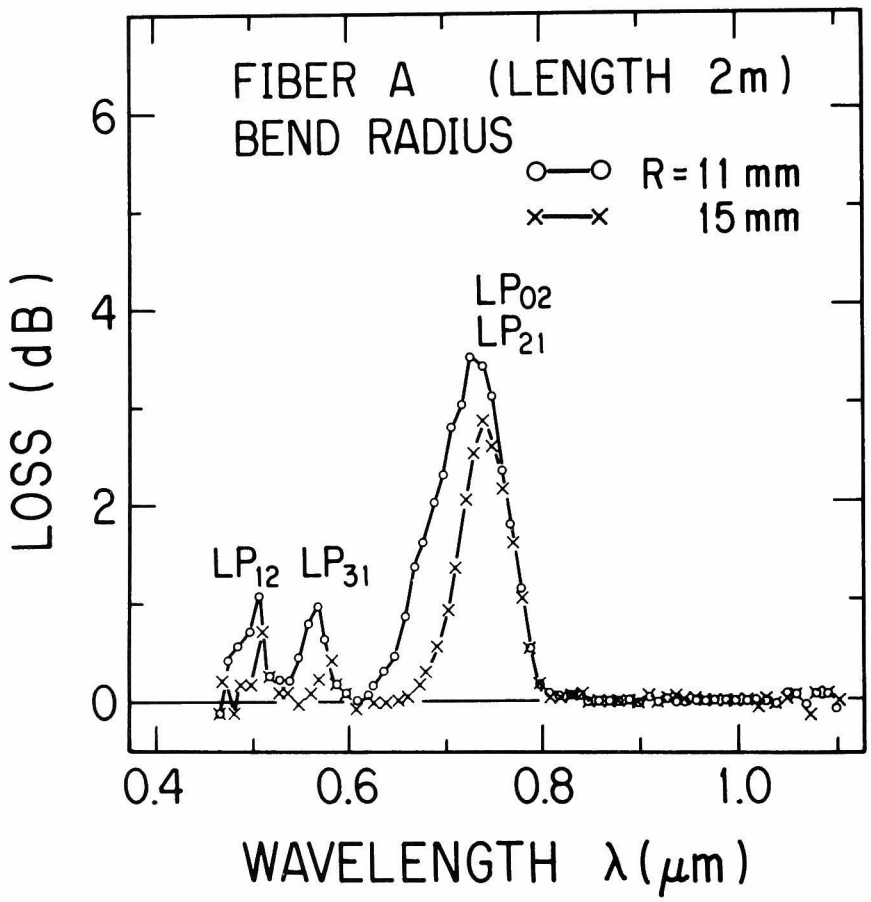

Fig. 2 Measured wavelength dependence of loss caused by circular bend for fiber A.

APPENDIX B HYDRAULIC PRESSURE DEPENDENCE OF OPTICAL LOSS IN JACKETED OPTICAL FIBER

Synopsis

Hydraulic pressure dependence of fiber loss is examined for several jacket structures. It is found that a liquid-filled pipe structure exhibits small loss increase, 0.9 dB/km at a pressure of 500 kg/cm^2, and is promising for use in a submarine optical cable.

An optical cable is considered to be a favoured transmission medium because of its several advantages over the conventional metallic conductor cables. It is interesting to develop a submarine optical cable, utilizing the merits inherent to fibers; low-loss, light weight, and small diameter. Transmission systems using the submarine optical cables are expected to have a long repeater spacing, since the low optica loss of the fibers is achieved now. Furthermore, if a light and slender submarine cable is realized, the cable can be easily installed under the sea.

However, since sea water, at great depth, applies high pressure to optical cables, it is necessary to examine the influence of hydraulic pressure on optical loss. In this section, we report experimental results obtained on optical loss hydraulic pressure dependence and discuss some possible structures of fiber jackets for use in a submarine optical cable.

Measurements of hydraulic pressure dependence were made by the following procedures. A measurement fiber was wound into a coil about 150 mm in diameter and was put into a 150 mm inner diameter pressure container. Two fiber ends were led out of the container through a small aperture, which was sealed with epoxy resin to

enable maintaining internal high pressure. The maximum pressure was chosen to be 500 kg/cm^2, which corresponds to a depth of 5000 meters under the sea. Loss measurements at each pressure were made thirty minutes after the pressure was applied, in order to remove influence due to creep. Step-index multimode fibers having a 40 μm core diameter, a 150 μm outer diameter, and a 0.76 % index difference were used. The test fibers had about 500 meter length and about 3 dB/km optical loss at a wavelength of 0.85 μm.

First, hydraulic pressure dependence of optical loss was measured for a bare fiber with an urethane primary coating several micrometers thick. Measured excess losses at a wavelength of 0.85 μm are shown in Fig. 1. It is found that the loss variation is less than ± 0.3 dB/km, which represents measurement accuracy. This experiment shows that guiding mechanism of optical power was not changed in the fiber by appling hydraulic pressure.

For optical cables, fibers are jacketed by plastics for protection. Several jacket structures were considered for a submarine optical cable, as shown in Fig. 2. Uniform hydraulic pressure is applied to the fiber through the jacket in structures A and B, and is applied

through liquid in structure C. It is expected, from the result shown in Fig. 1, that uniform pressure will not cause excess loss. In structure D, excess loss is simply prevented by isolating the fiber from hydraulic pressure with a pipe-shaped jacket.

The jacketed fibers shown in Fig. 2 were manufactured in order to examine their applicability to a submarine optical cable. Outer diameters of the jackets were about 1 mm. No excess loss, due to jacketing, was observed for any structures. Figure 3 shows the hydraulic pressure dependence of optical loss at a wavelength of 0.85 μm for four structures A - D. It is found that the loss increase is the largest in structure B. The excess loss at a pressure of 500 kg/cm^2 was about 3 dB/km in structure A and about 0.9 dB/km in structure C. In structure D, the jacket was broken at 400 kg/cm^2 and then the optical loss increased steeply. It is considered that the uniform pressure is applied to the fiber through liquid in structure C, resulting in very small excess loss. Another advantage of the structure is good pressure endurance. This fact is clearly seen, compared with the poor endurance in structure D.

The large loss increase, observed in structure A

and B, may be due to small irregularities in the plastic jacket which cause microbending [1] with increasing pressure. Excess losses measured were almost independent of optical wavelength. This is consistent with the spectral loss curves that Gardner showed in Reference 1. In order to discuss the excess loss due to pressure in comparison with that due to temperature change, optical loss was measured at low temperature for structures B and C. The loss variations for both structures were found to be less than the accuracy of the measurement in the temperature range between -60 and +60 °C. Thus, the hydraulic pressure has much greater influence on optical loss than the stress arising in the cooling process. It is presumed that the large excess loss due to pressure in structure B is originated from nonuniform contact at a boundary between the plastic jacket and the cushion layer. When the hydraulic pressure is applied, the fiber suffers nonuniform stress through the cushion layer. With increasing pressure above 300 kg/cm^2, the excess loss rather decreases. This fact is explained by a speculation that the nonuniformity is reduced at larger pressure. Hysteresis was observed in the loss/pressure relation in structure B. The speculation is consistent with this phenomenon. On the other hand, the nonuniform contact

does not influence the fiber loss when the temperature is lowered, because the cushion layer contracts radially almost in the same manner that the jacket does.

In conclusion, hydraulic pressure dependence of optical loss has been measured for several jacket structures. It is found that uniform hydraulic pressure does not cause excess loss and, consequently, excess loss is the smallest for structure C, liquid-filled pipe structure. Plastic adhesive structures, A and B, exhibit large loss increase, although stability to withstand temperature change is readily achieved. In order to decrease the excess loss for structures A - D, it is necessary to remove small irregularities existing in the plastic jacket. Establishment of jacketing technique is required for much more uniform jackets for structures A and B than for structure C, because plastic jacket contacts with fiber directly in structures A and B. At present. liquid-filled pipe structure C is considered to be suitable for a submarine optical cable.

Reference

1. W. B. Gardner: 'Microbending loss in optical fibers', Bell Syst. Tech. J., 54, 2, p.457 (1975)

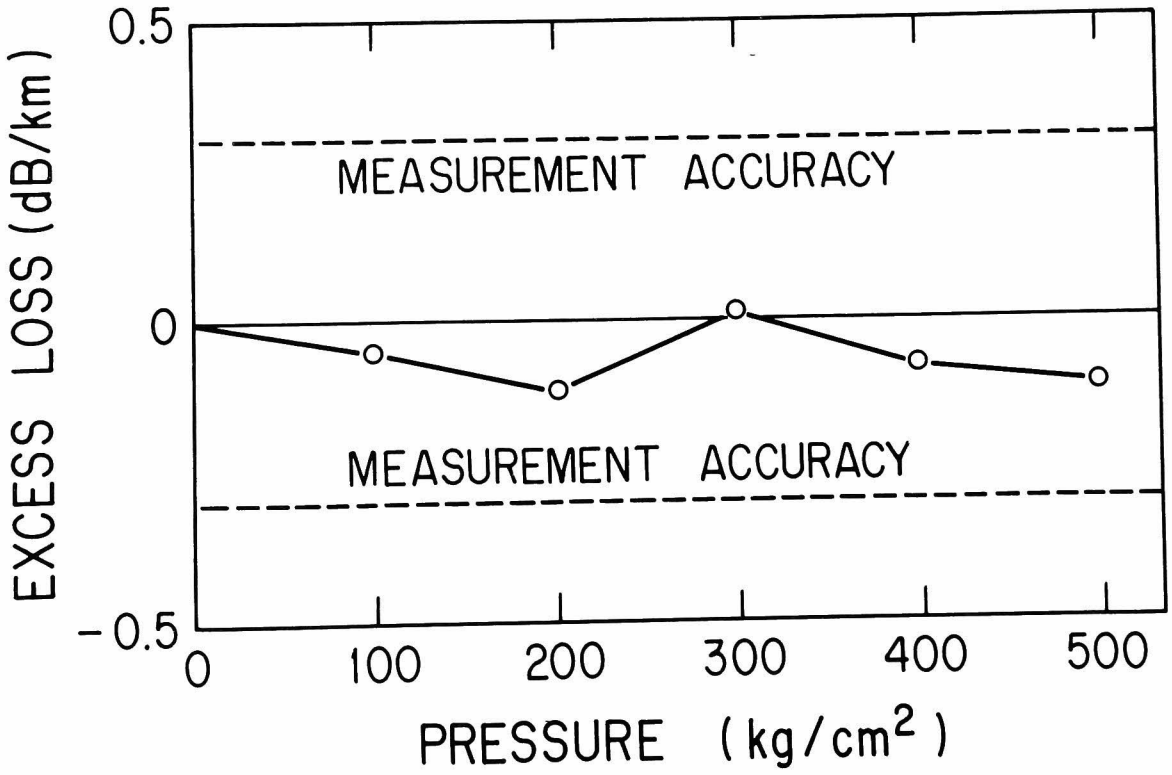

Fig. 1 Measured hydraulic pressure dependence of optical loss for bare fiber.

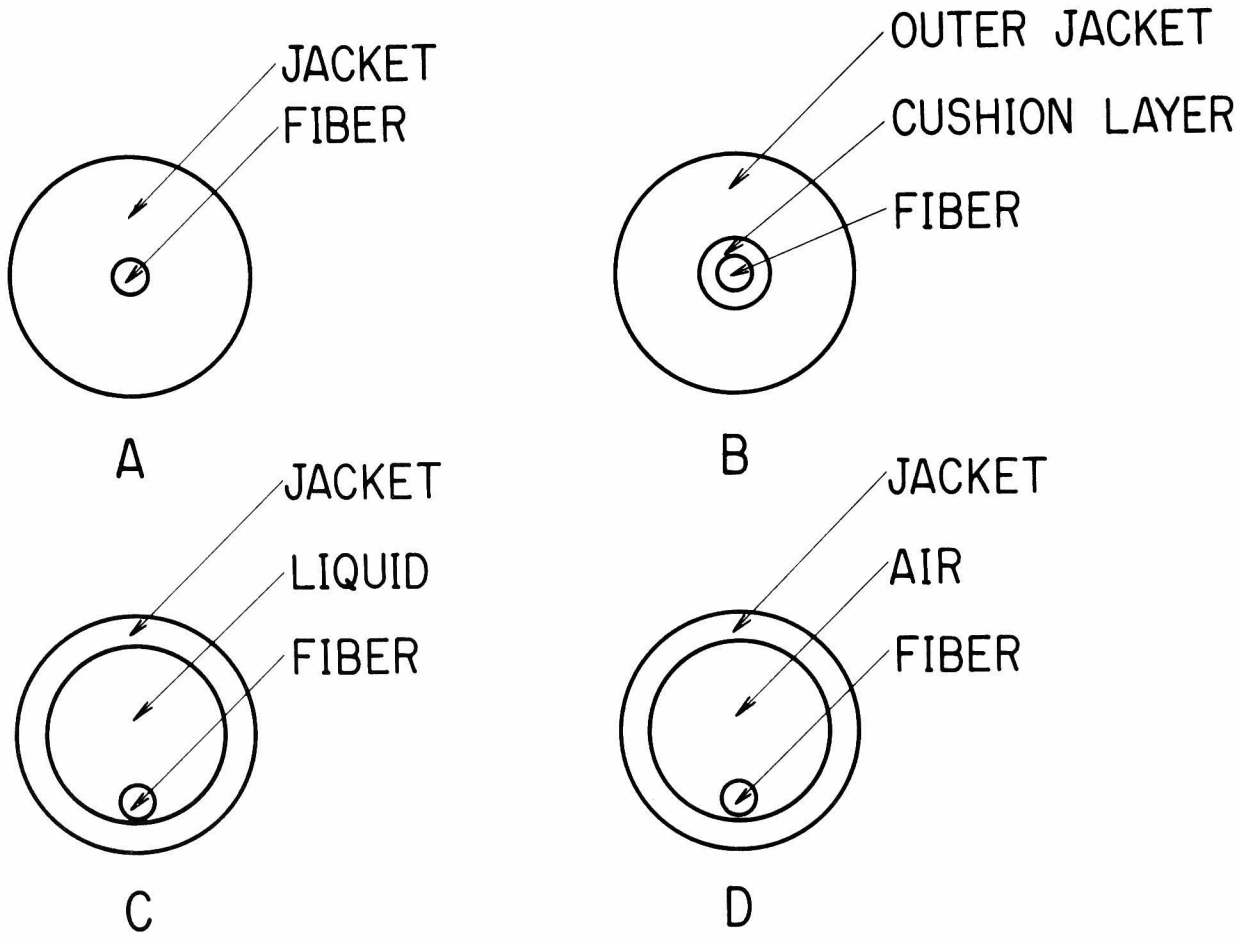

Fig. 2 Jacket structures for a submarine optical cable.

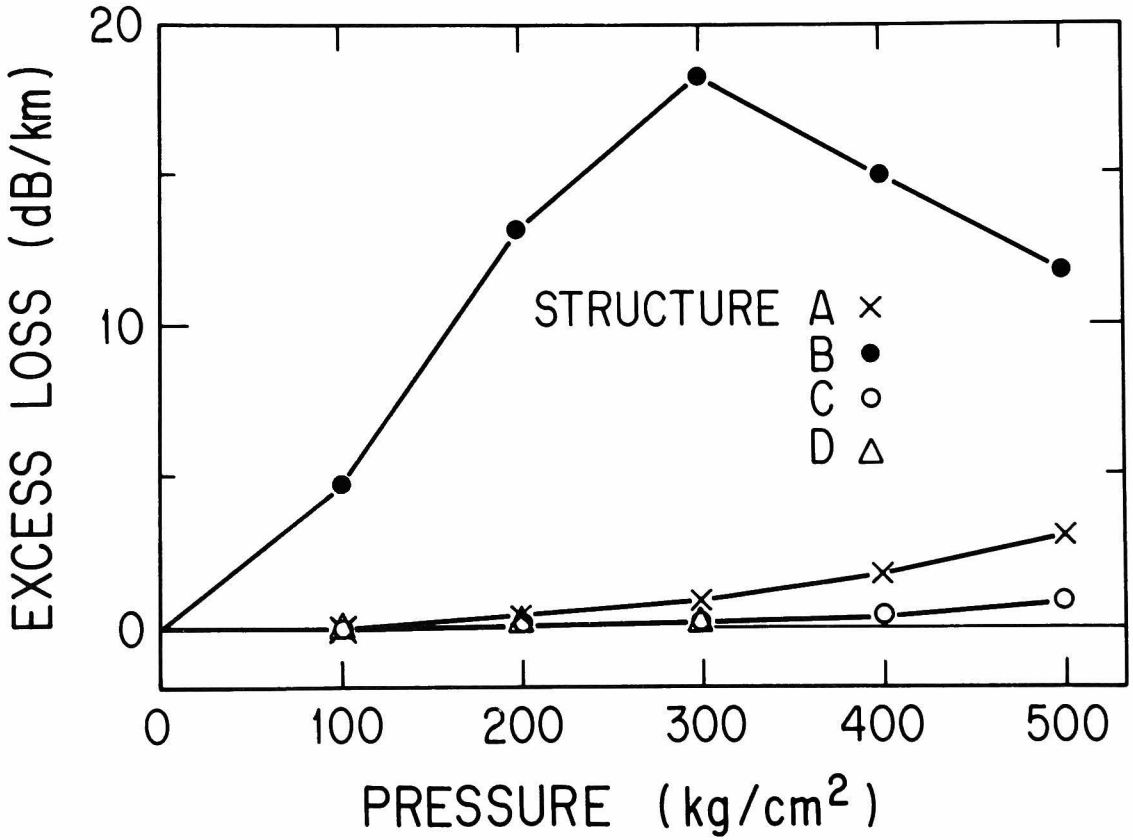

Fig. 3 Measured hydraulic pressure dependence of optical loss for jacketed fibers.

APPENDIX C SINGLE-MODE PROPAGATION IN 2-MODE REGION OF OPTICAL FIBER BY USING MODE FILTER

Synopsis

The effect of a mode filter using fiber bend has been clearly shown experimentally. The mode filter effectively removes the LP_{11} mode and has a negligibly small effect on the attenuation of the LP_{01} mode. The single-mode propagation was attained at the V-value of 2.8 by using the filter.

Introduction: Single-mode optical fiber is an attractive transmission medium, since it has broadband and low-loss transmission characteristics. It is important to determine suitable values for the fiber parameters, that is, the relative index difference Δ and core radius a, for constructing single-mode fiber cable transmission systems. Fiber parameters are required to satisfy a single mode condition, and in the case of step-index profile the condition is given by $V < 2.405$, where V is the normalized frequency (the so-called V-value).

It is preferable to select as large a V-value as possible, because loss increase due to cabling occurs in the small V-value region [1]. If the LP_{11} mode is removed by an adequate mode filter in the two-mode region ($V > 2.405$), single-mode propagation is also attained in this region. Thus, tolerance in V-value for single-mode fiber cable is expected to be large. Moreover, dispersion arising from the variation in group velocity V_g of the LP_{01} mode with wavelength λ falls to zero [2] at the V-value of approximately 2.9, and extremely wide bandwidth is expected by using a mode filter.

In this section, experimental results of a mode filter using fiber bend are described, and a limit of V-value for single-mode propagation is discussed.

Mode filter: Bending loss for the LP_{11} mode near the cutoff wavelength is much larger than that of the LP_{01} mode. Therefore, bending the fiber can produce a mode filter. The filter is set at the input side of the optical fiber, since only the LP_{01} mode is to be propagated in the fiber cable.

Experiments: The effect of the mode filter was examined for two kinds of fiber. Index differences and core diameters of the fibers were 0.3 % and 6.3 μm, respectively. The fiber length was 1.01 km. V-value is 2.7 at the optical wavelength of 0.82 μm. The filter was located at 3 meters from the input end of the fiber.

First, the effect of mode filter is demonstrated in Fig. 1. An optical pulse from a laser diode was transmitted, and two pulses corresponding to LP_{01} and LP_{11} modes are shown in Fig. 1 (a). Figure 1 (b) shows the elimination of the LP_{11} mode pulse using the mode filter. It is thus proved that the mode filter has a clear effect of LP_{11} mode elimination.

To evaluate the effect of the mode filter quantitatively, the optical loss was measured using an incoherent source and a monochromator. The optical power output from the fiber was detected with a Si P-I-N detector.

When mode coupling occurs of the LP_{01} to the LP_{11} mode after elimination of the LP_{11} mode, single-mode propagation cannot be attained. Therefore, existence of the LP_{11} mode, after passing through the mode filter, was examined in a fiber under random forces. The loss increase was measured while the fiber coils, which intersected each other, were held between two flat boards under a constant weight of 20 kg. Figure 2 shows the relation between loss increase due to the pressure and the bending radius R of the mode filter. The fiber with 150 μm outer diameter had 0.27 % relative index difference and 6.0 μm core diameter. The fiber was coated by silicone buffer, and the outer diameter was 0.4 mm. The fiber length was 460 meters. It is evident that the loss increase was due to the LP_{11} mode, because no loss increase was observed for the LP_{01} mode corresponding to single-mode propagation at V=2.4. The loss due to pressure decreased with decreasing bending radius of the filter. This is because the filter effectively removed the LP_{11} mode as the radius was decreased, and the LP_{11} mode was completely removed at R = 10 mm. These results also show that mode couplings to the LP_{11} mode are negligibly small, because no loss increase occurs after elimination of the LP_{11} mode. It is concluded that single-mode

propagation is attained using bending conditions: R = 10 mm, number of turns = 2.

The transmission system unavoidably contains splice points, and mode coupling at splice points must be examined. Figure 3 shows influence of splice point on loss increase due to pressure. Normalized frequency dependence of the loss increases was measured by changing the optical wavelength. The splice was made by an arc-fusion method, and the splice loss was 0.7 dB at the V-value of 2.4. No loss increase was observed when filtering the LP_{11} mode after its passage through the splice point. However, loss increase due to pressure did occur when the LP_{11} mode was filtered before it passed through the splice point. These results show that the mode coupling of the LP_{01} to the LP_{11} mode occurred at the splice point. It is therefore necessary to filter the LP_{11} mode after its passage through the splice point. In the future, low-loss splices without mode coupling must be studied.

Conclusions: The mode-filtering effect using fiber bend has been demonstrated. This mode filter has a simple structure and a clear effect. The filter removes the LP_{11} mode and has negligibly small effect on LP_{01} mode loss. It has become clear that single-mode propagation

is attained at the V-value of 2.8 by using the mode filter, and that the mode coupling of the LP_{01} to the LP_{11} mode was negligibly small, even under random forces.

References

1. Y. Katsuyama, Y. Ishida, K. Ishihara, T. Miyashita, and H. Tsuchiya: 'Suitable parameters of single-mode optical fibre', Electron. Lett., 15, 3, p.94 (1979)

2. W. A. Gambling, H. Matsumura, and C. M. Ragdale: 'Zero-mode dispersion in single-mode fibres', Electron. Lett., 14, 19, p.618 (1978)

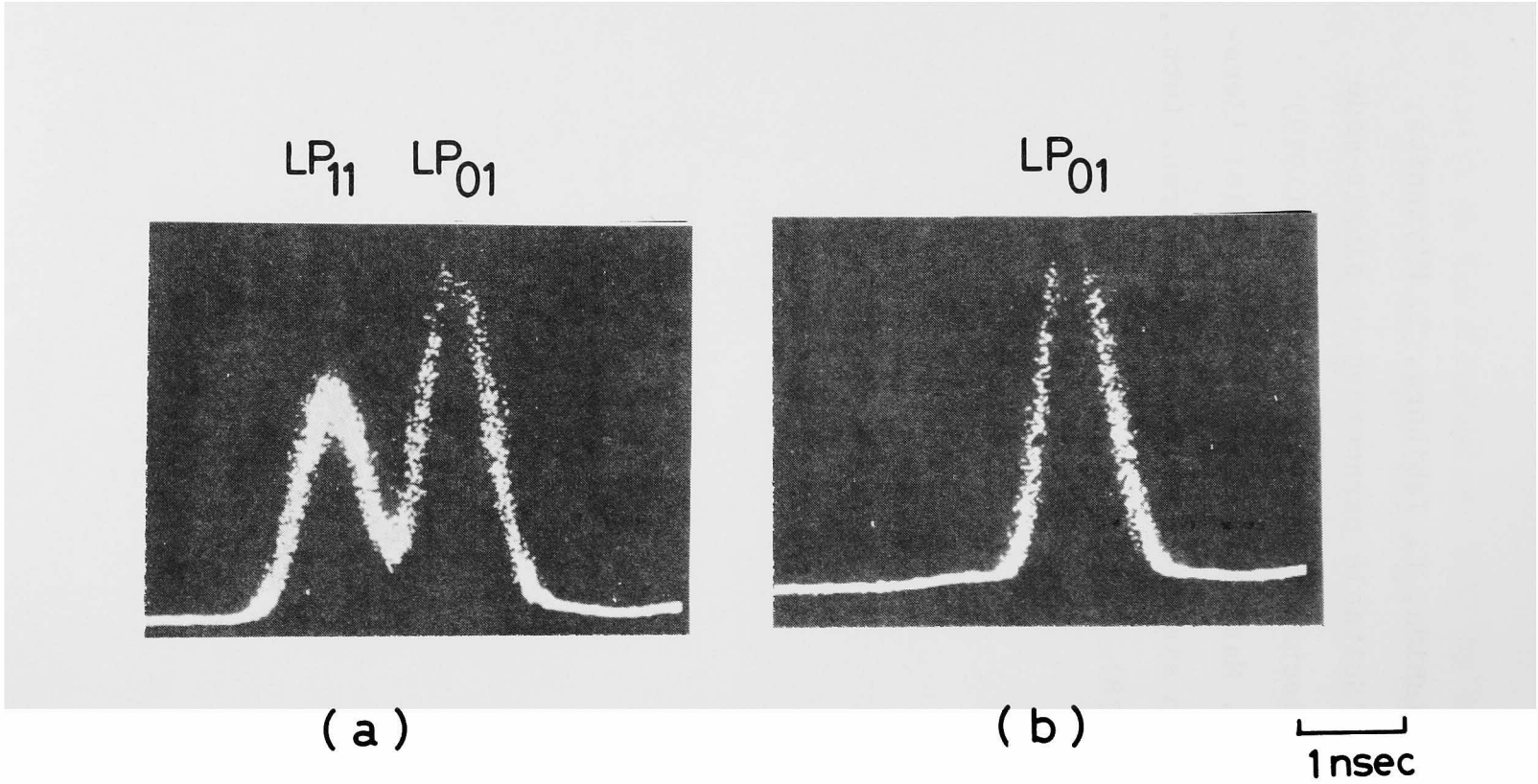

Fig. 1 Separated pulses due to time difference of transmission (a) without filter, and (b) with filter. Bending conditions are R = 10 mm and one turn. Index difference and core diameter of the fiber were 0.3 % and 6.3 μm, respectively. The fiber length was 1.01 km. V-value is 2.7 at the optical wavelength of 0.82 μm.

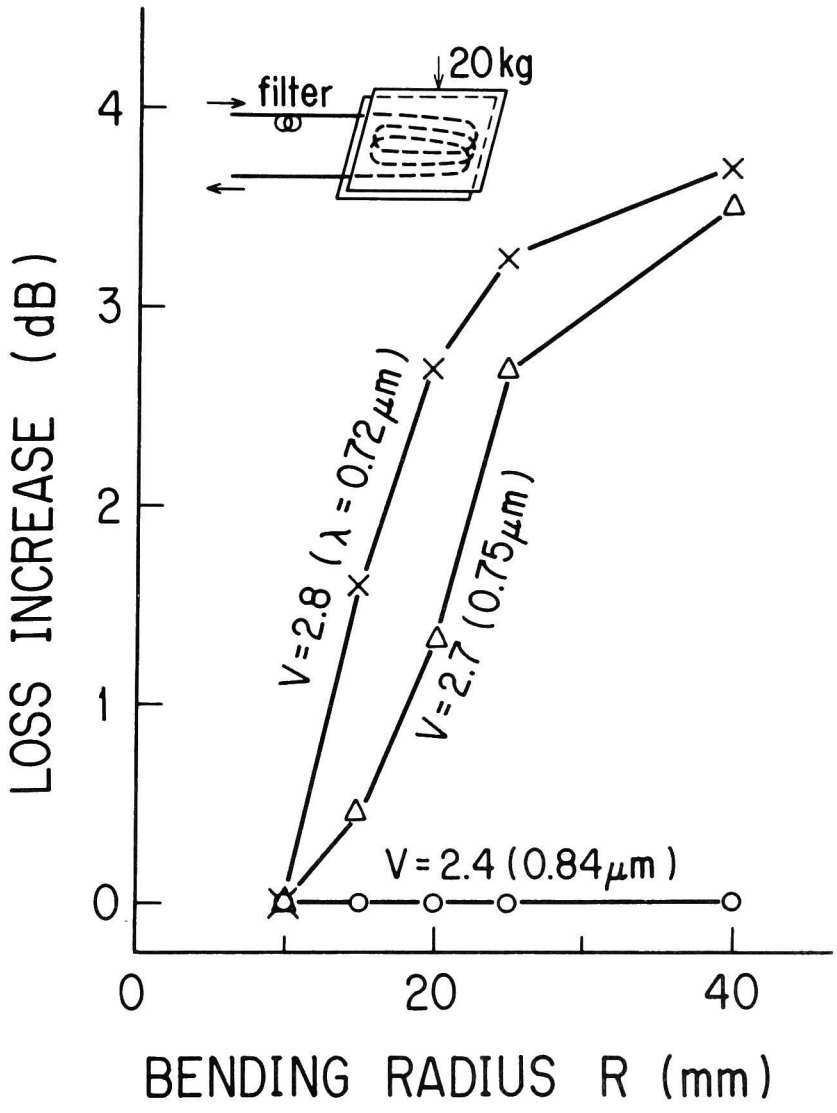

Fig. 2 Filter-bending-radius dependence of loss increase under random forces.
The number of turns is two.

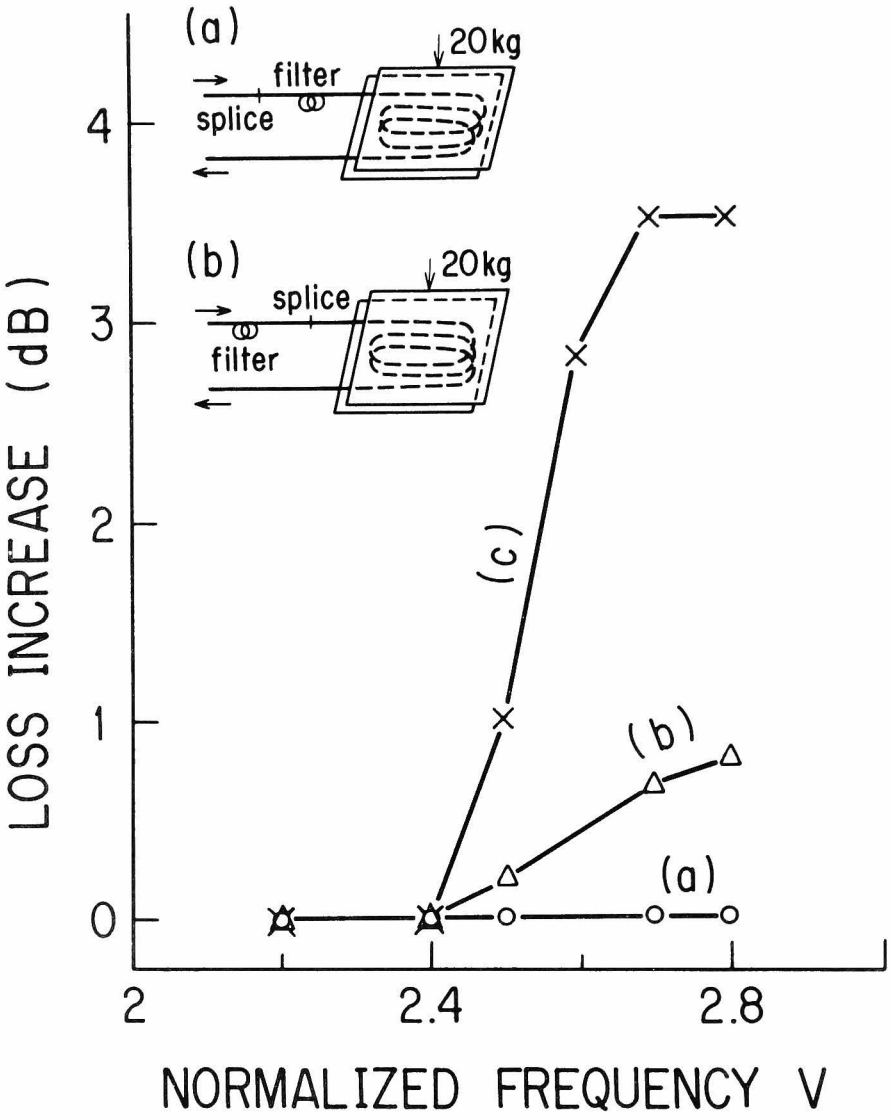

Fig. 3 Filter location related to splice point. The bending conditions are R=10 mm and two turns. (a) Filtering LP_{11} mode after passing through splice point. (b) Filtering LP_{11} mode before passing through splice point. (c) Without filtering.